Title

Pseudomonas aeruginosa Can Diversify after Host Cell Invasion to Establish Multiple Intracellular Niches

Journal

mBio, 13(6)

ISSN

2161-2129

Authors

Kumar, Naren G
Nieto, Vincent
Kroken, Abby R
et al.

Publication Date

2022-12-20

DOI

10.1128/mbio.02742-22

Peer reviewed

AMERICAN SOCIETY FOR MICROBIOLOGY | mBio®

RESEARCH ARTICLE

Pseudomonas aeruginosa Can Diversify after Host Cell Invasion to Establish Multiple Intracellular Niches

Naren G. Kumar,[a] Vincent Nieto,[a] Abby R. Kroken,[a]* Eric Jedel,[a] Melinda R. Grosser,[a]§ Mary E. Hallsten,[a] Matteo M. E. Mettrucio,[a] Timothy L. Yahr,[b] David J. Evans,[a,c] Suzanne M. J. Fleiszig[a,d]

[a]Herbert Wertheim School of Optometry & Vision Science, University of California, Berkeley, California, USA
[b]Department of Microbiology and Immunology, University of Iowa, Iowa, Iowa City, Iowa, USA
[c]College of Pharmacy, Touro University California, Vallejo, California, USA
[d]Graduate Groups in Vision Science, Microbiology, and Infectious Diseases & Immunity, University of California, Berkeley, California, USA

Naren G. Kumar and Vincent Nieto contributed equally to this article. The order was determined by the corresponding author after negotiation.

ABSTRACT Within epithelial cells, *Pseudomonas aeruginosa* depends on its type III secretion system (T3SS) to escape vacuoles and replicate rapidly in the cytosol. Previously, it was assumed that intracellular subpopulations remaining T3SS-negative (and therefore in vacuoles) were destined for degradation in lysosomes, supported by data showing vacuole acidification. Here, we report in both corneal and bronchial human epithelial cells that vacuole-associated bacteria can persist, sometimes in the same cells as cytosolic bacteria. Using a combination of phase-contrast, confocal, and correlative light-electron microscopy (CLEM), we also found they can demonstrate biofilm-associated markers: *cdrA* and cyclic-di-GMP (c-di-GMP). Vacuolar-associated bacteria, but not their cytosolic counterparts, tolerated the cell-permeable antibiotic ofloxacin. Surprisingly, use of mutants showed that both persistence in vacuoles and ofloxacin tolerance were independent of the biofilm-associated protein CdrA or exopolysaccharides (Psl, Pel, alginate). A T3SS mutant (Δ*exsA*) unable to escape vacuoles phenocopied vacuole-associated subpopulations in wild-type PAO1-infected cells, with results revealing that epithelial cell death depended upon bacterial viability. Intravital confocal imaging of infected mouse corneas confirmed that *P. aeruginosa* formed similar intracellular subpopulations within epithelial cells *in vivo*. Together, these results show that *P. aeruginosa* differs from other pathogens by diversifying intracellularly into vacuolar and cytosolic subpopulations that both contribute to pathogenesis. Their different gene expression and behavior (e.g., rapid replication versus slow replication/persistence) suggest cooperation favoring both short- and long-term interests and another potential pathway to treatment failure. How this intracellular diversification relates to previously described "acute versus chronic" virulence gene-expression phenotypes of *P. aeruginosa* remains to be determined.

IMPORTANCE *Pseudomonas aeruginosa* can cause sight- and life-threatening opportunistic infections, and its evolving antibiotic resistance is a growing concern. Most *P. aeruginosa* strains can invade host cells, presenting a challenge to therapies that do not penetrate host cell membranes. Previously, we showed that the *P. aeruginosa* type III secretion system (T3SS) plays a pivotal role in survival within epithelial cells, allowing escape from vacuoles, rapid replication in the cytoplasm, and suppression of host cell death. Here, we report the discovery of a novel T3SS-negative subpopulation of intracellular *P. aeruginosa* within epithelial cells that persist in vacuoles rather than the cytoplasm and that tolerate a cell-permeable antibiotic (ofloxacin) that is able to kill cytosolic bacteria. Classical biofilm-associated markers, although demonstrated by this subpopulation, are not required for vacuolar persistence or antibiotic tolerance. These findings advance our understanding of how *P. aeruginosa* hijacks host cells, showing

Editor Marvin Whiteley, Georgia Institute of Technology School of Biological Sciences

Address correspondence to Suzanne M. J. Fleiszig, fleiszig@berkeley.edu.

*Present address: Abby R. Kroken, Department of Microbiology and Immunology, Loyola University Chicago, Maywood, Illinois, USA.

§Present address: Melinda R. Grosser, Department of Biology, University of North Carolina, Asheville, North Carolina, USA.

The authors declare no conflict of interest.

This article is a direct contribution from Suzanne M. J. Fleiszig, a Fellow of the American Academy of Microbiology, who arranged for and secured reviews by Michael Schurr, University of Colorado School of Medicine, and Robert Shanks, University of Pittsburgh.

Received 7 October 2022
Accepted 13 October 2022
Published 14 November 2022

that it diversifies into multiple populations with T3SS-negative members enabling persistence while rapid replication is accomplished by more vulnerable T3SS-positive siblings. Intracellular *P. aeruginosa* persisting and tolerating antibiotics independently of the T3SS or biofilm-associated factors could present additional challenges to development of more effective therapeutics.

KEYWORDS antibiotic tolerance, biofilm, CdrA, epithelial cells, exoploysaccharides, imaging, intracellular bacteria, ofloxacin, *Pseudomonas aeruginosa*, type III secretion

Pseudomonas aeruginosa is a significant cause of morbidity and mortality, including burn-wound infections, septicemia, catheter-associated infections, corneal infections, community-acquired and nosocomial pneumonia, and chronic lung disease in persons with cystic fibrosis (CF). *P. aeruginosa* infections are notoriously difficult to treat due to a combination of inherent antimicrobial resistance and the versatility and adaptability of this opportunistic pathogen (1–5). While often considered an extracellular pathogen, several decades of work across many research labs have established that clinical isolates of *P. aeruginosa* can internalize and survive in host cells, including in animal models of infection (6–14). Despite this, surprisingly little is known about the intracellular lifestyle of *P. aeruginosa*, and many questions remain about how it contributes to disease pathogenesis and recalcitrance to therapeutics.

Previously, we showed that *P. aeruginosa* survival inside cells is modulated by the type III secretion system (T3SS) and several of its effectors (ExoS, ExoT, and ExoY), with ExoS playing a prominent role (11, 15, 16). While the RhoGAP activity of ExoS (and ExoT) can counter bacterial internalization by host cells via antiphagocytic activity (15, 17–20), bistability results in a lack of T3SS expression in many extracellular bacteria, effectively tempering antiphagocytic activity and allowing some population members to invade cells (11, 16, 21). Once inside the cell, efficient T3SS triggering allows expression of the T3SS, which in an ExoS-dependent manner inhibits vacuole acidification, enables escape from the endocytic vacuole, inhibits autophagy, and allows rapid replication of bacteria in the host cytosol (10, 17, 22, 23). Differing from other intracellular bacteria that use host cytoskeletal components for intracellular motility (24), *P. aeruginosa* then utilizes its own pili/twitching motility to disseminate throughout the host cell (25). Meanwhile, ExoS further supports intracellular survival by delaying lytic host cell death, effectively preserving the intracellular niche (16), and it drives formation of plasma membrane blebs to which some bacteria traffic and replicate within (9, 19). These blebs can subsequently disconnect from cells, becoming vesicles with intact membranes that can carry enclosed live/swimming bacteria to distant sites (9). Mutations affecting T3SS needle assembly, T3SS toxin secretion, or expression of the entire T3SS (Δ*exsA*) restrict intracellular bacteria to endocytic vacuoles (10, 11, 15), which we previously presumed were destined for degradation within lysosomes (10).

In a previous study, we showed that mutants defective in twitching motility, and therefore unable to disseminate intracellularly, formed nonmotile bacterial aggregates inside host cells surrounded by electron-lucid halos on electron micrographs (25). This led us to explore if *P. aeruginosa* was able to produce biofilm-associated factors inside infected host cells.

Biofilm formation has long been recognized as a strategy that bacteria use to survive under adverse environmental conditions, including during infections (26, 27). In human infections, *P. aeruginosa* biofilm formation can be associated with chronic persistence in the host, through a combination of phenotypic and genotypic adaptations that allow acquisition of essential nutrients and confer resistance to antimicrobial therapies and host defenses (28–31). Investigations of *P. aeruginosa* biofilm architecture and composition have revealed the presence of multiple bacterial exopolysaccharides in the biofilm matrix, including Psl, Pel, and alginate, the latter being most prominent in *P. aeruginosa* biofilms in CF (32, 33). CdrA is a bacterial protein with production regulated by the bacterial second messenger cyclic-di-GMP (c-di-GMP) that reinforces and protects the biofilm matrix (34, 35).

TABLE 1 *P. aeruginosa* strains, mutants, and plasmids used in this study

Name	Plasmid Origin of Replication	Description	Source/reference
Strains and mutants			
PAO1F		Wild type	Alain Filloux
PAO1FD*exsA*		*exsA* mutant	Alain Filloux
PAO1P		Wild type	Matthew Parsek (34)
PAO1PΔ*cdrA*		*cdrA* mutant	Matthew Parsek (34)
PAO1PΔ*EPS*		*psl*, *pel*, *algD* mutant	Matthew Parsek (34)
PAO1PΔ*EPS*Δ*cdrA*		*psl*, *pel*, *algD*, *cdrA* mutant	Matthew Parsek (32)
mPAO1		Wild type PAO1	*Pseudomonas* transposon library (72)
Plasmids			
pMG078	*pBBR1 oriV*	*cdrA*-GFP	This study
pFY4535		c-di-GMP TurboRFP reporter	Fitnat Yildiz (39, 40)
pJNE05	Plasmid: *pJN105*, ori: *pBBR1oriV*	T3SSGFP expression vector (pJNE05::*exoS*-GFP)	Timothy Yahr (73)
pBAD-GFP ($pGFP_{arabinose}$)	Plasmid: *pJN105*, ori: *pBBR1oriV*	Arabinose-inducible GFP (pTJ1::araGFP)	This study
pMG055	Plasmid: pTJ1, ori: *oriT*	Constitutive blue fluorescent protein (EBFP2)	This study

Extracellular DNA (eDNA) is another major component of the biofilm matrix that interacts with polysaccharide components and can modulate bacterial dispersal (36–38).

To test the hypothesis that intracellular *P. aeruginosa* could demonstrate biofilm-associated markers, we used gene expression reporters for *cdrA* encoding the biofilm-matrix protein and c-di-GMP (which triggers biofilm formation). Results for both corneal and bronchial epithelial cells showed distinct intracellular populations when cells were infected with wild-type *P. aeruginosa*, with *cdrA*-expressing bacteria localized to vacuoles and T3SS-expressing bacteria in the cytosol, often in the same cell. The data also showed potentially important functional differences between the two populations, with cytosolic *P. aeruginosa* being sensitive to the cell-permeable antibiotic ofloxacin, and vacuolar populations demonstrating ofloxacin tolerance even at high concentrations. Surprisingly, neither persistence in vacuoles nor ofloxacin tolerance required *cdrA* or any of the three exopolysaccharides (*alg*, *psl*, *pel*) known to be associated with biofilm formation. Raising potentially interesting implications for the impact of antibiotics on infection pathogenesis, the results also showed that the vacuole-located antibiotic survivors were able to trigger cell death.

The discovery that *P. aeruginosa* can establish niches in multiple locations within the same epithelial cells (cytoplasm, membrane blebs, vacuoles) differs from other bacterial pathogens which traffic to either vacuoles or the cytoplasm in a linear fashion. The finding that the bacteria in these alternate locations express different survival/virulence determinants and vary in antibiotic susceptibility predicts a "covering of the bases" for the overall population. Interestingly, this pattern of gene expression occurring simultaneously in infected cells is reminiscent of the acute versus chronic infection expression phenotypes, which are generally thought to represent entirely different infection types. How intracellular diversification relates to those previously described infection phenotypes, and the relevance of these results to antibiotic treatment failure *in vivo*, will require further investigation.

RESULTS

Bacteria expressing biofilm-associated factors *cdrA* and c-di-GMP localize to vacuoles in human epithelial cells. To determine if biofilm-associated factors were expressed by intracellular *P. aeruginosa*, human corneal and bronchial epithelial cells were imaged 6 h after inoculation with *P. aeruginosa* organisms that report expression of *cdrA* (pMG078) or c-di-GMP (pFY4535) (39, 40) (Table 1). Results were compared to those of bacteria that instead report T3SS expression (10, 11). Following a 3-h infection period to allow bacteria to invade cells, extracellular bacteria were eliminated using the non-cell-permeable antibiotic amikacin, thereby allowing intracellular bacteria to be selectively visualized (8, 10, 11).

Aligning with our previously published data (9–11, 16), T3SS-expressing intracellular

bacteria localized to the cytosol in both epithelial cell types, wherein they replicated rapidly and disseminated throughout the cytoplasm (Fig. 1). Bacteria expressing the biofilm-associated factors *cdrA* or c-di-GMP were also detected among the intracellular population. Rather than being in the cytosol, this subpopulation appeared to be contained in vacuole-like niches that remained stable over time (Fig. 1A). To confirm that *cdrA*-green fluorescent protein (GFP)-reporting bacteria (pseudocolored red) were within vacuoles as opposed to being in aggregates within the cytosol, real-time phase-contrast microscopy was used to visualize the cellular compartment in which they were contained. Figure 1B shows *cdrA*-GFP-reporting PAO1F (11, 16, 21) located in vacuoles in corneal epithelial cells, and Fig. 1C shows the same PAO1F phenotype in bronchial epithelial cells. A different wild-type parental strain PAO1P (35, 41) (see Table 1) also showed the same *cdrA*-GFP-reporting vacuole-located phenotype within corneal epithelial cells (data not shown). Thus, for two PAO1 parental wild types, some of the subpopulation expressing *cdrA* was found restricted within membrane-bound circular phase-clear regions, implicating vacuoles and distinguishing them from possible intracellular cytosolic aggregates.

Having shown distinct intracellular phenotypes of *P. aeruginosa*, the percentage of corneal epithelial cells containing *cdrA*-expressing intracellular bacteria was then quantified. Cells were infected with PAO1F expressing the *cdrA*-GFP reporter (pMG078), and total intracellular bacteria were detected with an anti-*Pseudomonas* antibody at 6 h post-infection (Fig. 1D). The percentage of cells containing intracellular bacteria that expressed only *cdrA* (*cdrA*^{on}) was quantified, along with the percentage of cells containing intracellular bacteria not expressing *cdrA* (*cdrA*^{off}) and those containing both. Of 520 cells analyzed, 7.7% contained only *cdrA*-expressing bacteria (red bar), and 9.6% contained *cdrA*^{off} bacteria (green bar), while 6% contained both phenotypes (yellow bar) (Fig. 1D). Images below the quantitative data show examples of each of these different categories.

To determine if a lack of vacuolar escape into the cytosol necessarily leads to *cdrA* expression, we performed the same analysis using a mutant lacking ExsA, the transcriptional activator of the T3SS (PAO1FΔ*exsA*) (9). This mutant does not express the T3SS and remains in vacuoles because the T3SS is required for vacuolar escape and survival in the cytosol (10). Results (Fig. 1E) confirmed that at this time point (6 h postinfection), *exsA* mutants were present only in vacuoles and that the percentage of cells containing internalized bacteria was similar to the wild-type parent PAO1F (see Fig. 1D). Importantly, the distribution of *cdrA*^{on} versus *cdrA*^{off} bacteria found in vacuoles for *exsA* mutant-infected cells (Fig. 1E) was similar to that for wild-type-infected cells (see Fig. 1D). Images of the *cdrA*^{on} and *cdrA*^{off} categories for *exsA* mutant-infected cells are shown (Fig. 1E).

Thus, both wild-type bacteria and T3SS (*exsA*) mutants can express *cdrA* when in vacuoles, and this occurs in a similar percentage of the infected host cell population under these experimental conditions.

Vacuolar localization does not require *cdrA*. C-di-GMP is a trigger for biofilm formation, while CdrA is the only known biofilm matrix protein made by *P. aeruginosa*. Since *cdrA* was expressed only in bacteria localized to vacuoles, we next asked if vacuolar localization depends on CdrA, and potentially also on biofilm formation. Thus, we compared a *cdrA* mutant (PAO1PΔ*cdrA*) to the wild type (PAO1P) for the ability to persist in vacuoles. First, we confirmed that the *cdrA* mutant did not differ from the wild type in its ability to invade corneal epithelial cells (Fig. 2A) and did not have a different impact on cell viability over time (data not shown). Next, we compared the percentage of corneal epithelial cells that contained at least one *cdrA*-GFP-expressing bacterium after infection with the wild type (PAO1P) or *cdrA* mutant (PAO1PΔ*cdrA*) at 6 h postinfection. Results showed that the *cdrA* mutant and wild type trafficked to vacuoles in a similar percentage of cells over the 6-h period (Fig. 2B). Phase-contrast microscopy also showed that mutants unable to express *cdrA* (Δ*cdrA*) trafficked to vacuoles at 6 h post-infection (Fig. 2C). This further shows that vacuolar persistence at 6 h post-infection did not require CdrA (Fig. 2B and C).

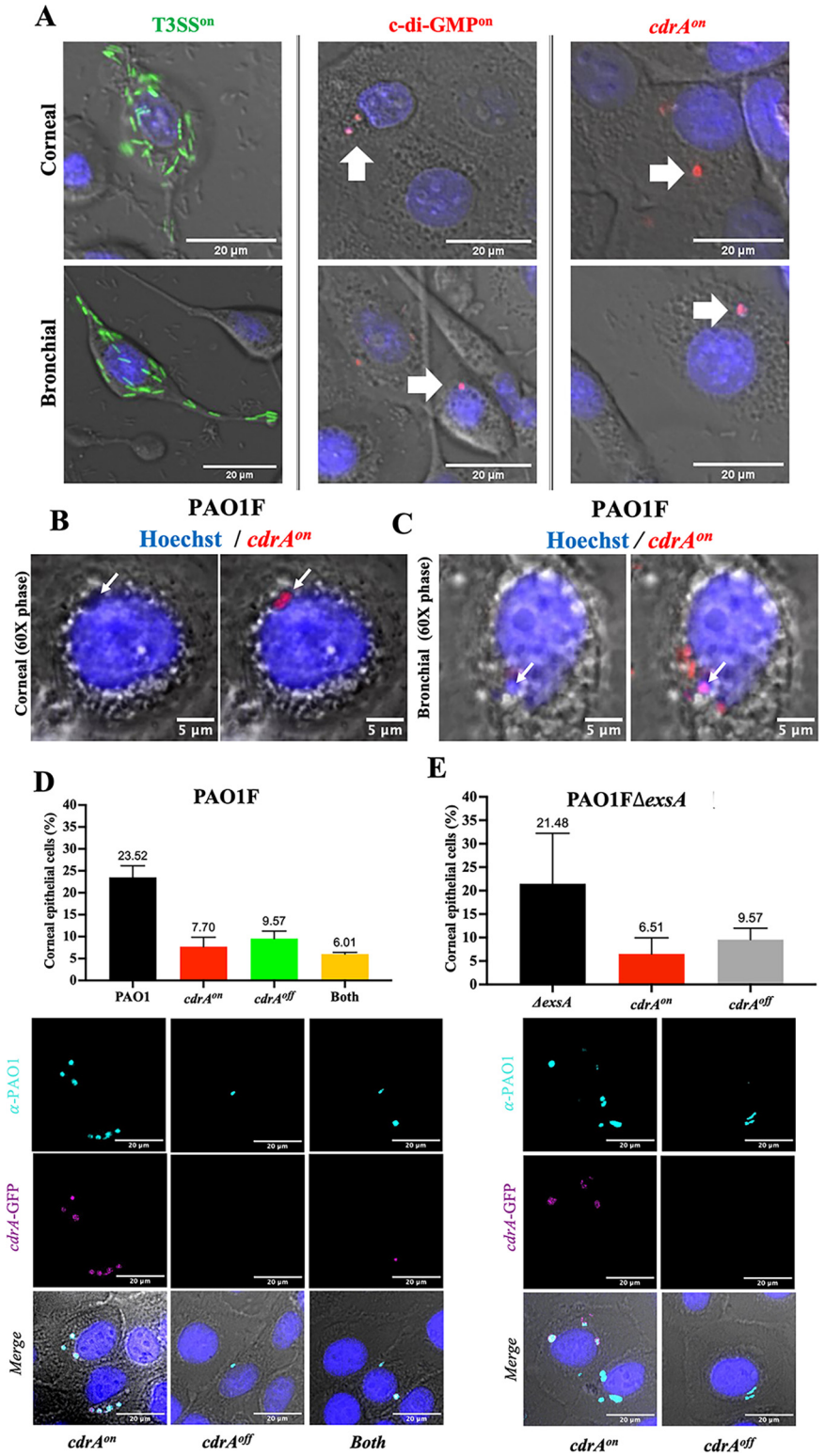

FIG 1 Intracellular wild-type *P. aeruginosa* form distinct phenotypes within human epithelial cells. (A) Intracellular expression of genes encoding the T3SS (green), chronic switch regulator c-di-GMP (red), or biofilm matrix protein CdrA (*cdrA*-GFP, pseudocolored red) in human corneal or bronchial epithelial cells at 6 h postinfection with *P. aeruginosa* PAO1F. Extracellular bacteria were killed at 3 h postinfection with amikacin (200 μg/mL). T3SS-expressing bacteria occupied the cytosol as expected. In contrast, bacteria reporting c-di-GMP or *cdrA* expression formed distinct localized vacuole-like niches within the same or different cells. (B and C) Oil-immersion phase-contrast microscopy shows *cdrA*-GFP-reporting bacteria (pseudocolored red puncta) of wild-type PAO1F localized to vacuoles in corneal epithelial cells

(Continued on next page)

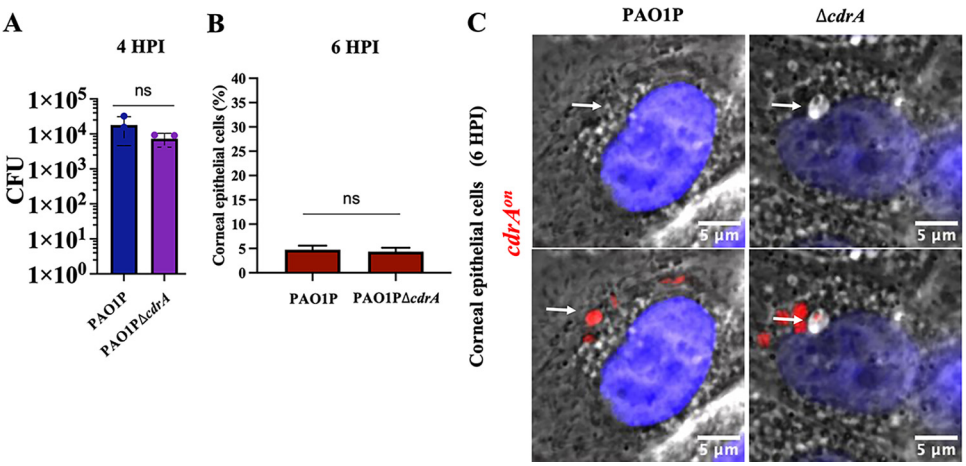

FIG 2 CdrA is not required for host cell invasion and vacuolar localization. (A) Invasion of corneal epithelial cells quantified by quantifying CFU (CFU) at 4 h postinfection. Corneal cells were infected for 3 h with PAO1P and PAO1PΔ*cdrA*. Extracellular bacteria were killed 3 h postinfection with amikacin (200 μg/mL) and cells lysed to recover intracellular bacteria. (B) Percentage of human corneal epithelial cells containing at least one *cdrA*^{on} bacterial cell at 6 h postinfection. (C) Oil-immersion phase-contrast microscopy shows *cdrA*-expressing bacteria (red puncta) of wild-type PAO1P and its mutant PAO1PΔ*cdrA* localized to vacuoles in corneal or bronchial cells. White arrows point to bacteria in vacuoles. The same image is shown with and without fluorescence. ns, not significant (Student's *t* test).

Among intracellular bacteria, the *cdrA*-expressing population is more tolerant to ofloxacin than the T3SS-expressing population. Biofilm-associated bacteria tend to be more antibiotic tolerant. Thus, we next explored if the intracellular *cdrA*-expressing population could resist an antibiotic better than their cytosolic T3SS-expressing cell-mates. This was done using ofloxacin, an antibiotic differing from amikacin (in part) by being able to penetrate host cell membranes. Wild-type bacteria were allowed to internalize for 3 h before exposing epithelial cells to either amikacin alone (non-cell permeable, kills only extracellular bacteria) or amikacin plus ofloxacin (to additionally target intracellular bacteria). Ofloxacin concentrations were chosen according to the MIC for the PAO1 strain variants used (see Materials and Methods). For PAO1F, the MIC for ofloxacin was determined to be 0.25 μg/mL, and for that reason the concentrations used ranged from 0.25 to 4 μg/mL (1× to 16× MIC). Figure 3 shows time-lapse imaging of intracellular *P. aeruginosa* gene expression using T3SS-GFP and *cdrA*-GFP reporters and the percentage of epithelial cells containing at least one GFP-positive bacterial cell at 6 and 12 h postinfection.

Cytosolic T3SS^{on} populations showed significant susceptibility to ofloxacin at 1 μg/mL (4× MIC) at both 6 h and 12 h, with fewer infected cells detected over time (Fig. 3A to C and Video S1 in the supplemental material). In contrast, intracellular *cdrA*^{on} bacteria continued to report with ofloxacin treatment concentrations all the way up to 4 μg/mL (16× MIC) at both 6 and 12 h postinfection, with ~ 4 to 6% of epithelial cells containing *cdrA*^{on} bacteria (Fig. 3D to F and Video S2). These results showed that vacuolar *cdrA*-

FIG 1 Legend (Continued)
(B) or bronchial epithelial cells (C). (D) Percentage of corneal epithelial cells containing any intracellular *P. aeruginosa* (PAO1F, black bar) and distinct *cdrA*-expressing phenotypes. After labeling all bacteria with anti-*Pseudomonas* antibody, *cdrA*-GFP reporter expression allowed subdivision of invaded cells into those only containing *cdrA*^{on} bacteria (red bar), only *cdrA*^{off} (green bar), and both *cdrA*^{on} and *cdrA*^{off} (yellow bar). (E) Percentage of corneal epithelial cells containing intracellular PAO1FΔ*exsA* (black bar), a T3SS mutant that only localizes to vacuoles (9). Cells containing *exsA* mutants showed a vacuolar distribution similar to that of the wild type with some only containing *cdrA*^{on} (red bar) and others containing *cdrA*^{off} vacuolar bacteria (gray bar). In panels D and E, there was no significant difference between subgroups in the distribution of vacuolar phenotypes (one-way ANOVA with Dunnett's multiple-comparison test). Data are shown as the mean ± SD of three biological replicates. Images below the quantitative data in panels D and E show examples of corneal epithelial cells for each of the categories quantified (bacteria pseudocolored as indicated: *cdrA*-GFP, magenta; anti-*Pseudomonas* antibody, cyan).

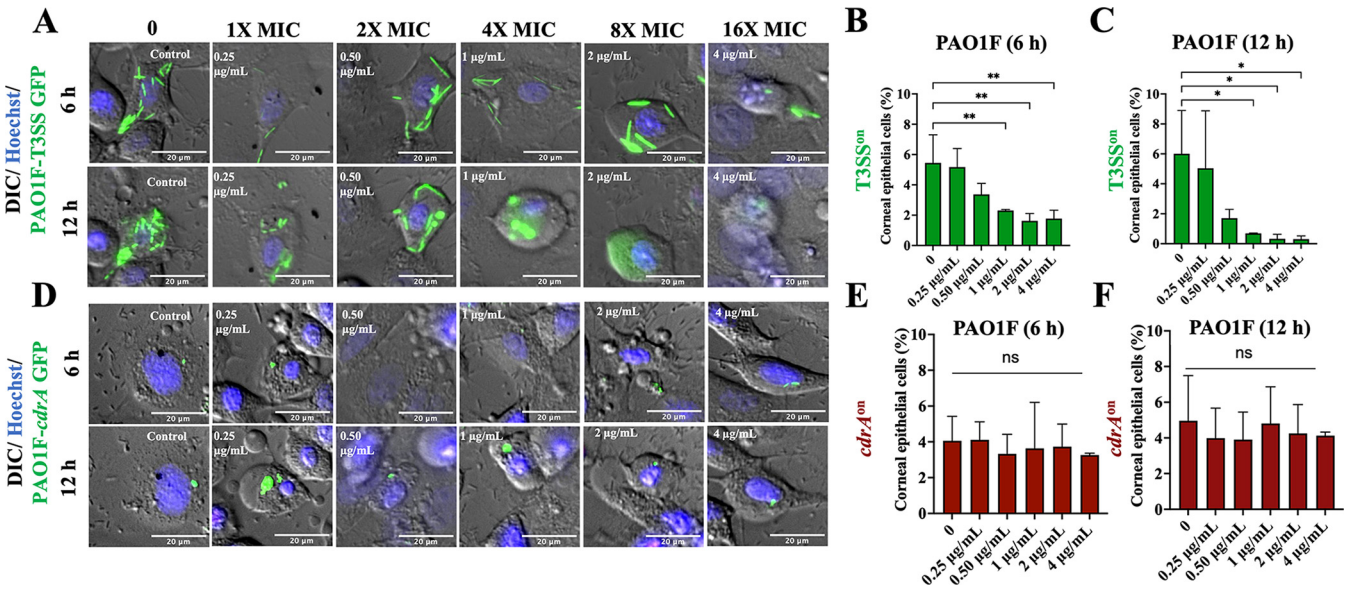

FIG 3 Vacuolar *cdrA*^{on} populations show resistance to the cell-permeable antibiotic ofloxacin compared to cytosolic T3SS^{on} bacteria. (A) Images of human corneal epithelial cells containing cytosolic T3SS-GFP-expressing PAO1F (T3SS^{on}) in the presence of ofloxacin (0.25 to 4 μg/mL = 1 to 16× MIC) at 6 h and 12 h postinfection versus control. Extracellular bacteria were killed after 3 h with the non-cell-permeable amikacin (200 μg/mL) (control), or amikacin (200 μg/mL) and ofloxacin were added at 3 h to also target intracellular bacteria. (B and C) Percentage of corneal epithelial cells containing at least one T3SS^{on} bacterial cell at 6 h (B) and 12 h (C) postinfection under the above-described conditions. Increasing concentrations of ofloxacin eliminated most cytosolic bacteria (*, $P < 0.05$; **, $P < 0.01$; ns, not significant; one-way ANOVA with Dunnett's multiple-comparison test). (D) Images of *cdrA*-GFP-expressing PAO1F vacuolar bacteria (*cdrA*^{on}) in the presence of ofloxacin as described above. Discrete foci of bacteria (green) persisted at 16× the MIC of ofloxacin and at 12 h postinfection. (E to F) Percentage of human corneal epithelial cells containing at least one *cdrA*^{on} bacterial cell at 6 h (E) and 12 h (F) postinfection under the above-described conditions. Increasing concentrations of ofloxacin failed to eliminate the *cdrA*^{on} vacuolar population. There was no significant difference between groups (one-way ANOVA with Dunnett's multiple-comparison test). Data are shown as the mean ± SD of three biological replicates.

expressing bacteria were better able to resist killing by ofloxacin than T3SS-reporting cytosolic bacteria in the same infected host cell population.

Correlative light-electron microscopy confirmed viability and vacuolar localization of ofloxacin-tolerant *P. aeruginosa*. Since the fluorescent signal from intracellular bacteria may persist long after bacterial cell death (42) and *cdrA* expression is induced upon cell contact, correlative light-electron microscopy (CLEM) was used to confirm that *cdrA*-GFP-reporting bacteria surviving above MICs of ofloxacin were both intracellular and localized to vacuoles. CLEM is essentially a combination of wide-field immunofluorescence and electron microscopy (EM) using the same section to localize fluorescence with morphological details (e.g., of a cell) (43, 44). Ofloxacin was used at 6 h post-infection (with PAO1F) at a concentration that can clear the cytosolic population (1 μg/mL, see Fig. 3A). Figure 4 shows three individual cells containing *cdrA*-GFP-expressing bacteria in vacuoles, all localized to the perinuclear region where late endosomes are expected to reside, each containing ~1 to 4 bacterial cells. Since vacuole-localized bacteria have intact cell walls after antibiotic treatment, this suggests that vacuole-localized populations are viable. This outcome supports the conclusion from our wide-field fluorescence and differential interference contrast (DIC)/phase-contrast microscopy experiments (Fig. 1A and B; Fig. 2C; Fig. 3D) that ofloxacin-tolerant *cdrA*-expressing subpopulations can be intracellular *P. aeruginosa* and that they localize to vacuoles.

Detectable *cdrA* expression does not correlate with ofloxacin resistance. While the experiments described above show that *cdrA*-expressing intracellular bacteria localized to vacuoles, not all vacuole-located bacteria expressed *cdrA*. Heterogeneity among vacuolar bacteria is not surprising, as they likely transition through various phenotypes after internalization/replication and as maturation of the vacuole alters their environment. Here, we sought to explore ofloxacin susceptibility among all vacuolar bacteria in a wild-type infection, not just those expressing *cdrA*. To specifically label all intracellular bacteria and study the effect of ofloxacin on the total population of

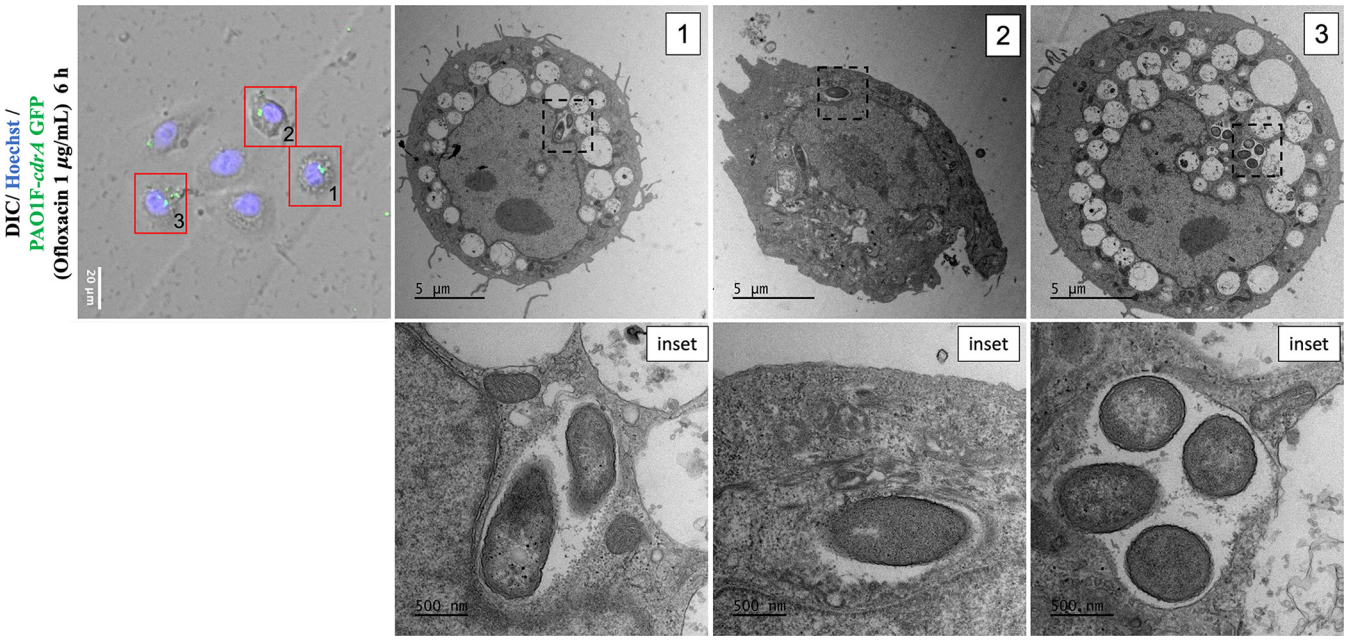

FIG 4 Correlative light-electron microscopy of *cdrA*^{on} bacteria in vacuoles. Fluorescence and electron micrographs of human corneal epithelial cells at 6 h after inoculation with PAO1F expressing *cdrA*-GFP. Extracellular bacteria were killed 3 h postinfection with amikacin (200 μg/mL), and amikacin (200 μg/mL) and ofloxacin (1 μg/mL) were then added for a further 3 h. Cells were fixed at 6 h, and fluorescence microscopy was performed before preparing cells for electron microscopy (EM). Red boxes show corneal epithelial cells with corresponding EM micrographs. Black dotted boxes indicate regions from which the respective insets were taken to show bacteria within vacuoles with evidence of vacuolar membranes.

intracellular bacteria, ofloxacin was used to kill the susceptible population in cells infected with wild-type bacteria expressing an arabinose-inducible reporter ($pGFP_{arabinose;}$ see Materials and Methods and Fig. S1) where only the survivors express GFP. Epithelial cells containing at least one ofloxacin survivor were then quantified at 6 and 12 h (Fig. 5). As expected, when ofloxacin was not used or was used only at sublethal concentrations (less than the MIC of 0.50 μg/mL), epithelial cells infected with wild-type bacteria were found to contain both cytosolic and vacuole-localized bacteria (Fig. 5A). When ofloxacin was used 2 times above the MIC (0.5 μg/mL) or higher, there was a gradual reduction in the number of cytosolic bacteria, while only vacuolar populations continued to persist (Fig. 5A). The percentage of cells containing vacuoles with ofloxacin-tolerant bacteria was similar at 6 h (Fig. 5B) and 12 h (Fig. 5C), showing stability during the intervening time. Comparison to the percentage of cells containing any ofloxacin survivors in vacuoles to those containing only *cdrA*^{on} survivors (~10%, Fig. 5B and C versus ~4%, Fig. 3E and F) suggested additional ofloxacin-tolerant bacteria (in vacuoles) besides those expressing *cdrA* (Fig. 5A versus Fig. 3D). These results suggested that while vacuolar bacteria can express *cdrA* and can also tolerate high doses of ofloxacin, expression of *cdrA* is dispensable for vacuolar localization and tolerating high concentrations of the antibiotic (Fig. 2C). Unfortunately, experiments to test this more directly could not be done using bacteria simultaneously expressing both reporters (i.e., arabinose-inducible GFP and *cdrA*) because expression of dual-fluorescent reporters in *P. aeruginosa* impairs bacterial fitness and affects the invasion of host cells. Instead, we used isogenic *cdrA* mutants as discussed below.

CdrA and biofilm-associated EPS is dispensable for ofloxacin resistance of vacuolar *P. aeruginosa*. Having shown expression of the biofilm-associated gene *cdrA* in a subset of vacuolar bacteria, along with vacuolar bacteria being more tolerant to ofloxacin than cytosolic bacteria, and having shown that ofloxacin-tolerant bacteria could express *cdrA*, we next explored if CdrA was required for ofloxacin resistance of vacuolar bacteria. To more broadly study the contribution of biofilm formation, we also considered biofilm-associated exopolysaccharides (EPS). Thus, mutants in CdrA (Δ*cdrA*), exopolysaccharides (Δ*EPS*; *psl*, *pel*, and alginate), or both (Δ*cdrA*/Δ*EPS*) were tested for

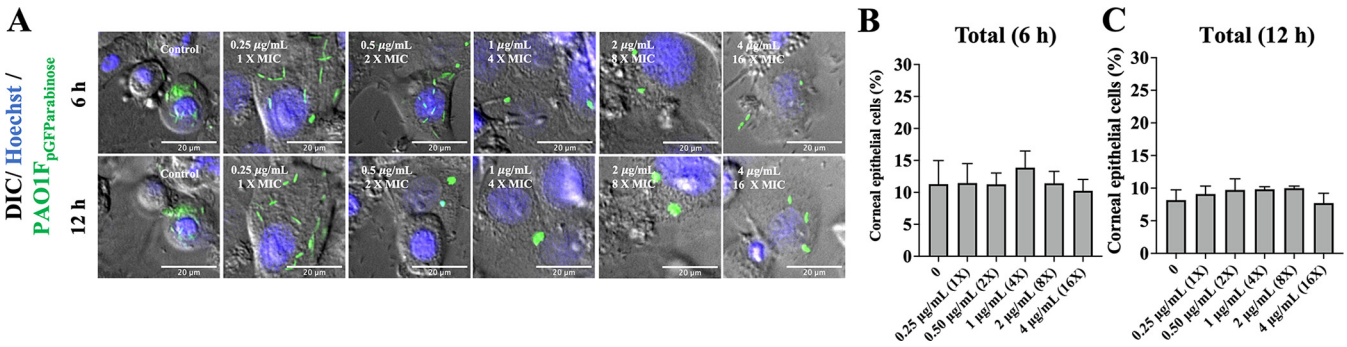

FIG 5 The total population of ofloxacin-tolerant wild-type *P. aeruginosa* localizes to vacuoles. (A) Images of human corneal epithelial cells containing PAO1F expressing $pGFP_{arabinose}$ to show all intracellular bacteria in the presence of ofloxacin (0.25 to 4 μg/mL = 1 to 16× MIC) at 6 and 12 h postinfection versus control. After 3 h extracellular bacteria were killed with amikacin (200 μg/mL) (control), or amikacin (200 μg/mL) and ofloxacin were added to also target intracellular bacteria. Cytosolic PAO1F were cleared by ofloxacin at 1 μg/mL at 6 h and by 0.5 μg/mL at 12 h. Vacuolar bacteria persisted in the epithelial cells at 12 h postinfection at all ofloxacin concentrations. (B and C) Percentage of corneal epithelial cells containing at least one PAO1 with $pGFP_{arabinose}$ bacterial cell at 6 h (B) and 12 h (C) post-infection under the above-described conditions. Despite ofloxacin clearance of cytosolic bacteria, the percentage of cells containing intracellular bacteria did not significantly differ between the control and ofloxacin-treated groups (one-way ANOVA with Dunnett's multiple-comparison test). Data are shown as the mean ± SD of three biological replicates.

intracellular ofloxacin resistance using time-lapse imaging as described above. Since the *in vitro* MIC of PAO1P (the wild-type parent of these mutants) was 4 μg/mL, versus 0.25 μg/mL for PAO1F (used above), the ofloxacin concentration was adjusted accordingly from 0 to 64 μg/mL (0 to 16× MIC). Figure 6A to D shows the percentage of corneal epithelial cells containing at least one GFP-expressing bacterial cell at 12 h post-infection. Use of $pGFP_{arabinose}$ detected all viable intracellular *P. aeruginosa*, while *cdrA*-GFP specifically

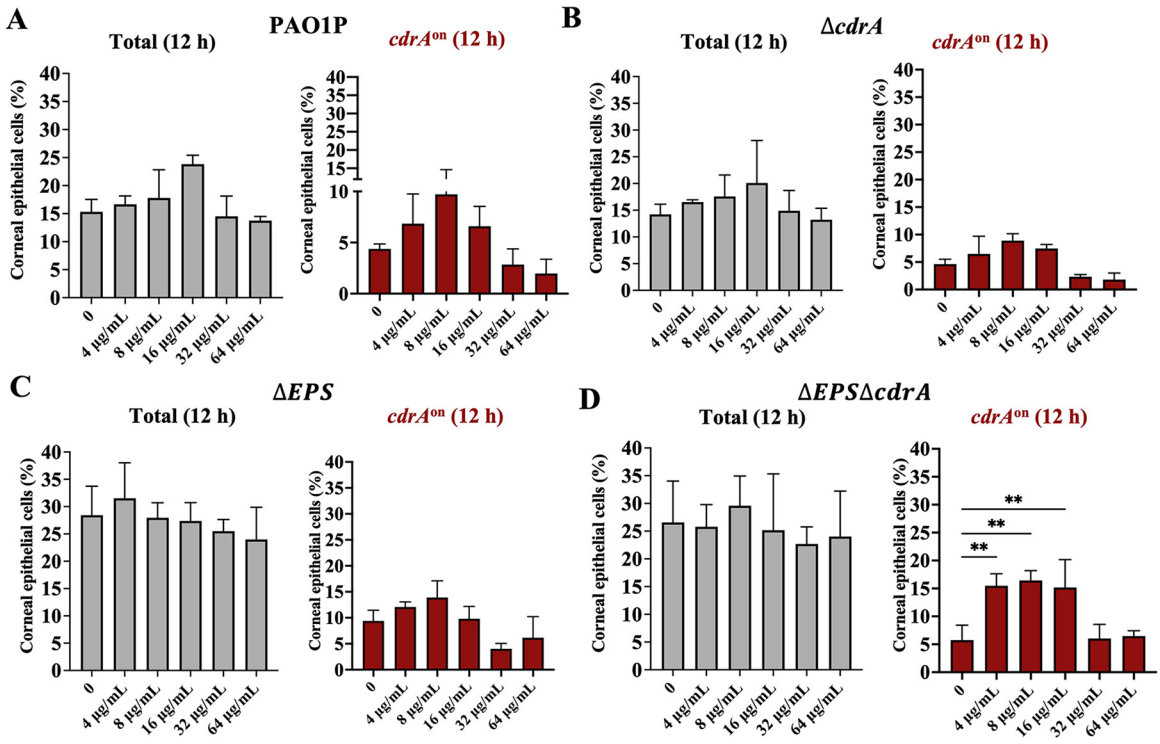

FIG 6 Ofloxacin resistance of vacuolar *P. aeruginosa* does not require *cdrA* or exopolysaccharide. (A to D) Percentage of human corneal epithelial cells containing intracellular *P. aeruginosa* at 12 h postinfection with (A) PAO1P, (B) PAO1PΔ*cdrA*, (C) PAO1PΔEPS (Δ*pel*Δ*psl*Δ*algD*), or D) PAO1PΔEPSΔ*cdrA*. Total intracellular bacteria were detected using $pGFP_{arabinose}$ (gray bars), and vacuolar $cdrA^{on}$ bacteria were detected using *cdrA*-GFP (red bars). Extracellular bacteria were killed after 3 h with amikacin (200 μg/mL) and with amikacin (200 μg/mL) and ofloxacin added at 3 h (4 to 64 μg/mL = 1 to 16× MIC). Intracellular bacteria persisted up to 16× MIC for the wild type and mutants, with a subset of each expressing *cdrA*. *, $P < 0.05$; **, $P < 0.01$; ***, $P < 0.001$; ****, $P < 0.0001$ (one-way ANOVA with Dunnett's multiple-comparison test versus untreated control). Data are shown as the mean ± SD of three biological replicates.

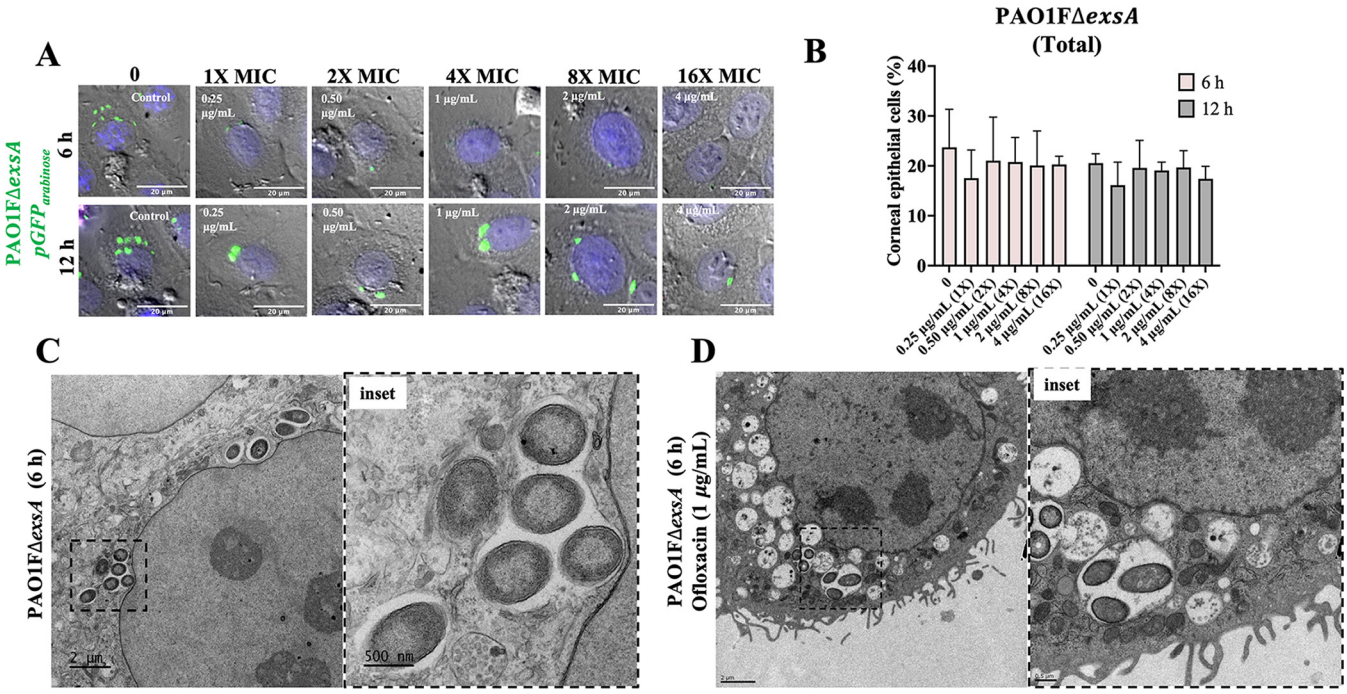

FIG 7 Vacuolar T3SS (Δ*exsA*) mutants are also tolerant to ofloxacin. (A) Images of corneal epithelial cells containing PAO1FΔ*exsA* ($pGFP_{arabinose}$) show that all intracellular bacteria are localized to vacuoles with or without ofloxacin (0.25 to 4 μg/mL = 1 to 16× MIC) at 6 and 12 h postinfection. Extracellular bacteria were killed after 3 h with amikacin (200 μg/mL), and then amikacin (200 μg/mL) and ofloxacin were added for a further 3 h. (B) Percentage of corneal epithelial cells containing at least one bacterial cell at 6 h and 12 h postinfection under the above-described conditions. Increasing concentrations of ofloxacin failed to eliminate the *exsA* mutant vacuolar population at either time point. There was no significant difference between groups (one-way ANOVA with Dunnett's multiple-comparison test). (C and D) Correlative light-electron microscopy to visualize *exsA* mutants in vacuoles in the corneal epithelial cells at 6 h postinfection in control (C) and ofloxacin-treated (1 μg/mL) (D) cells under the same conditions. Both insets show bacteria restricted to perinuclear vacuoles with evidence of a vacuolar membrane.

reported biofilm-associated subpopulations. Surprisingly, there was no significant difference between wild-type and *cdrA* mutants in the number of cells still containing viable intracellular bacteria after ofloxacin treatment at all concentrations up to 64 μg/mL (16× MIC) (Fig. 6A and B), with each strain entering ~15 to 20% of the corneal epithelial cells (Fig. 6A and B, gray bars) and *cdrA*-GFP expressing vacuolar subpopulations in ~5 to 10% of those cells (Fig. 6A and B, red bars). This was shown using arabinose-inducible GFP to detect all intracellular ofloxacin survivors and the *cdrA* reporter to detect only the subset reporting *cdrA* promoter activity (which still occurs in *cdrA* mutants) (Fig. 6B). Thus, *cdrA* is not required for the ofloxacin resistance exhibited by vacuolar *P. aeruginosa*, in addition to not being required for vacuolar localization.

As shown in Fig. 6C and D, similar results were obtained for the Δ*EPS* triple mutant lacking all three biofilm-associated exopolysaccharides (EPS) and a quadruple mutant additionally lacking CdrA (Δ*EPS* Δ*cdrA* mutant). In each case the percentage of epithelial cells containing *cdrA* promoter-expressing vacuolar subpopulations at each ofloxacin concentration was similar.

Control experiments confirmed that PAO1F and PAO1P showed similar levels of internalization into human corneal epithelial cells at 4 h postinfection, as did PAO1P relative to its *cdrA* and *EPS* mutants (Fig. S2).

T3SS mutants unable to exit vacuoles show similar ofloxacin resistance to vacuole-located wild-type PAO1. The above-described data suggested that something about vacuolar localization might promote ofloxacin resistance, independently of expression of classical biofilm-associated factors (e.g., CdrA and EPS) that coincidentally occur in that location, possibly even a physical feature of the vacuole itself rather than a bacterium-driven mechanism. As a first step toward understanding this, we used a T3SS mutant (PAO1FΔ*exsA*) unable to escape the vacuoles (9–11, 17). Figure 7 shows time-lapse imaging of human corneal epithelial cells infected with PAO1FΔ*exsA*

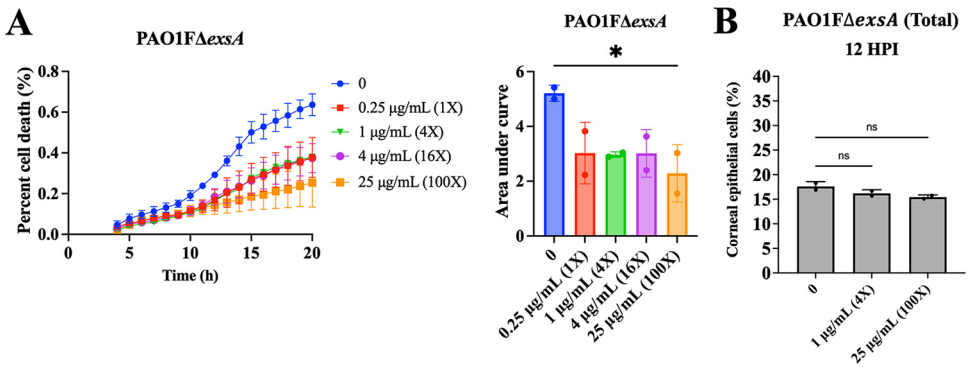

FIG 8 Vacuolar *P. aeruginosa* contributes to host cell death. Quantification of corneal epithelial cell death quantified using the ratio of propidium iodide (PI)/Hoechst, also shown as the area under the curve (AUC) after internalization of *P. aeruginosa* PAO1FΔ*exsA* (A) from 4 to 20 h postinfection. Extracellular bacteria were killed after 3 h with non-cell-permeable amikacin (200 μg/mL), and ofloxacin was added at 3 h (0.25 to 25 μg/mL = 1 to 100 $\times$ MIC) with continued amikacin. Intracellular survival of bacteria is shown as the percentage of corneal epithelial cells containing a GFP-expressing bacterium (pGFP$_{arabinose}$) treated with 0 (no ofloxacin), 1 μg/mL (4$\times$ MIC), or 25 μg/mL (100$\times$ MIC) at 12 h postinfection (B). The data show that ofloxacin-sensitive and ofloxacin-tolerant vacuolar bacteria both contribute to host cell death. *, $P < 0.05$; ns, not significant (one-way ANOVA with Dunnett's multiple-comparison test versus untreated control).

expressing pGFP$_{arabinose}$ to visualize all intracellular bacteria over time with and without ofloxacin and subsequently quantify the percentage of cells containing internalized bacteria. As expected, the Δ*exsA* mutant localized only to vacuoles observed as GFP-expressing puncta within the epithelial cells that increased in fluorescence over time (Fig. 7A). This population survived exposure to ofloxacin at 6 and 12 h postinfection (Fig. 7B, Video S3). CLEM was then used to ensure that persistent vacuolar populations were due to live bacteria and not residual GFP signal from dead bacteria (42). Results showed that the Δ*exsA* mutant localized to perinuclear vacuoles with multiple bacteria in a single membrane-bound compartment (Fig. 7C, inset). Some of these vacuolar bacteria were seen surviving exposure to ofloxacin (1 μg/mL) as shown by bacteria maintaining their cell wall integrity in perinuclear vacuoles (Fig. 7D, inset). Thus, T3SS mutants of *P. aeruginosa* that cannot escape vacuoles can phenocopy the T3SS-off subpopulation of the wild type when infecting corneal epithelial cells with respect to tolerating ofloxacin, supporting the possibility that vacuolar localization itself enables survival.

Vacuolar-localized *P. aeruginosa* can drive host cell death. The above-described experiments showed that vacuolar bacteria can be more tolerant to ofloxacin. To further explore the significance of the vacuolar phenotype, we next examined how it impacts the host cell. Using the same experimental protocols as described above, the kinetics of human corneal epithelial cell death during infection were measured using propidium iodide. After cells were infected with PAO1Δ*exsA* (occupies only vacuoles) for 3 h, extracellular bacteria were killed using amikacin (200 μg/mL), and then ofloxacin, 0 to 4 μg/mL (0 to 16$\times$ MIC), was added into the medium to also kill the cytosolic population. Cells containing intracellular bacteria showed increasing cell death from 4 to 24 h up to a maximum of ~40% of the total population, the kinetics not significantly affected by ofloxacin exposure up to 4 μg/mL (16$\times$ MIC) (Fig. 8A). A significant reduction in cell death was only observed when the ofloxacin concentration was increased to 25 μg/mL (100$\times$ MIC). While 25 μg/mL (100$\times$ MIC) of ofloxacin did not reduce visible GFP expression (pGFP$_{arabinose}$) (Fig. 8B), the effect on cell death suggests supraphysiological concentrations of antibiotic are required to inactivate vacuole-localized populations. This further suggests an active role of intracellular vacuolar bacteria in the outcome of host cell death.

Diversification of intracellular phenotypes also occurs during *in vivo* corneal infection. It has been 3 decades since we initially reported that *P. aeruginosa* can invade corneal epithelial cells *in vivo* in mice, including the first observation that they

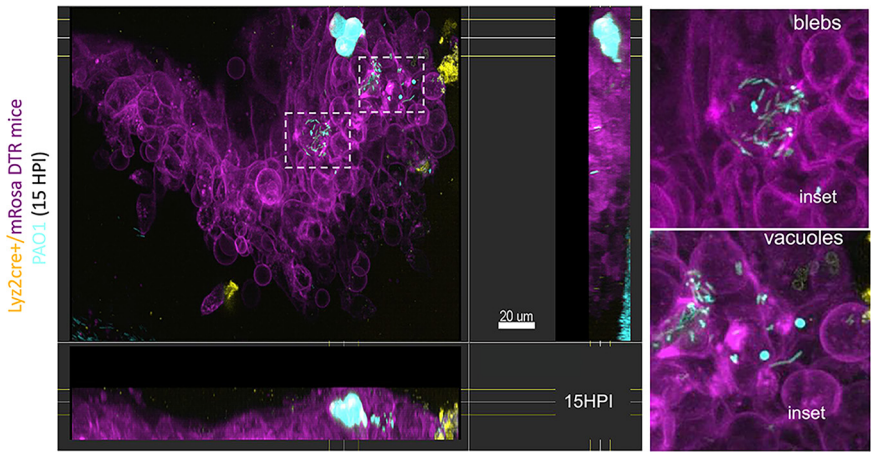

FIG 9 Intracellular cytosolic and vacuolar phenotypes of *P. aeruginosa* both occur *in vivo* during corneal infection. Corneal image of a Lyz2cre+/mRosa-DTR mouse (red fluorescent membranes with green/yellow myeloid-derived cells) at 15 h postinfection with *P. aeruginosa* mPAO1 expressing pMG055 (EBFP2 [blue], pseudocolored cyan) using the murine scarification model. Confocal images were taken in the middle of the infected cornea scratch on an anesthetized live mouse. Insets show cytosolic bacteria spreading in the cell and/or within membrane blebs and vacuolar bacteria (blue puncta) within neighboring cells. Side panels show lateral projections of imaging into the epithelium.

could be in membrane-bound vacuoles as shown using transmission electron microscopy (TEM) (6). Because TEM required sample fixation, it was unclear if these bacteria were destined to be degraded, to enter the cytoplasm, or to persist in the vacuoles.

More recently, we used intravital confocal imaging without fixation to confirm *in vivo* that when *P. aeruginosa* enters the cell cytosol it can colonize the cytoplasm or can traffic to membrane blebs (45). Since the present study revealed intracellular diversification leading to cytosolic and vacuolar bacteria coexisting in the same infected cell population *in vitro*, we next asked if this could also occur *in vivo*. To explore this, we used a murine scarification model that enables *P. aeruginosa* to colonize the epithelium. This was done using Lyz2cre+/mRosa-DTR mice that constitutively express a red fluorescent protein in their cell membranes along with green/yellow myeloid-derived cells and infecting these mice with mPAO1 constitutively expressing blue-fluorescent protein (pMG055). In this way, we were able to study the localization of infecting bacteria relative to the host cell membranes and differentiate myeloid- and non-myeloid-derived cell types in the cornea. Live confocal imaging at 15 h post-infection showed three intracellular phenotypes similar in appearance to our *in vitro* observations. These included both cytoplasmic and membrane bleb-contained *P. aeruginosa*, in addition to intracellular aggregates appearing to be vacuoles containing bacteria.

The absence of tissue fixation/sectioning allowed us to additionally collect temporal data in 3D in intact eyes during infection. Doing so, we were able to observe *in vivo* multiple phenomena that we have reported when *P. aeruginosa* infects cultured corneal and other epithelial cells. This included a subpopulation in the cytosol demonstrating twitching motility, a second subpopulation demonstrating swimming motility inside plasma membrane blebs, and a third population stationary and appearing to be confined to vacuoles (Fig. 9, Videos S4 to S6). These results suggest that all of the intracellular phenomena that we have reported when *P. aeruginosa* infects cultured cells occur during infection *in vivo*.

DISCUSSION

Bacteria surviving inside host cells generally orchestrate their localization and replication via secretion of virulence factors to establish a niche in either the cytosol or subcellular membrane-bound compartments such as vacuoles, secretory vesicles, and endoplasmic reticulum (46–49). Previously, we showed that when *P. aeruginosa* invades

epithelial cells, it can utilize its type III secretion system (T3SS) to escape vacuoles (17). This is followed by rapid replication and dissemination throughout the cytosol, with the T3SS effector ExoS used to avoid autophagy and to construct and occupy host cell plasma membrane blebs (9, 11, 19). We have also reported that *P. aeruginosa* differs from other pathogens by not depending on host cell cytoskeletal elements for intracellular motility, with bacteria instead using their own appendages (25). This includes pilus-driven twitching motility in the cytoplasm and flagella-mediated swimming motility within membrane blebs (11).

The T3SS of *P. aeruginosa* is expressed by only some population members even under inducing conditions (11, 50). Since the T3SS is required for vacuolar escape but not cell entry, T3SS-off subpopulation members remain in vacuoles after being internalized (9–11). Our prior model was that these were destined for degradation in lysosomes, an idea supported by vacuole acidification (10). Here, we instead found that T3SS-off *P. aeruginosa* remained viable over long periods of time in vacuoles, shown using both corneal and bronchial epithelial cells. We also found they could differentiate into a phenotype expressing biofilm-associated factors that are not expressed by their cytoplasmic counterparts. These vacuolar T3SS-off bacteria were often present in cells also containing cytosolic T3SS-on bacteria. Thus, we have identified a novel (third) intracellular niche for *P. aeruginosa* inside epithelial cells in which the bacteria are in a different phenotypic state (T3SS-off, biofilm-producing, nonmotile) in addition to being in a different intracellular location (vacuoles). Use of CLEM to simultaneously study the fine structure of the host cells versus location of CdrA-expressing bacteria confirmed that this biofilm protein was expressed by intracellular bacteria residing in vacuoles.

The significance of *P. aeruginosa* residing in epithelial cell vacuoles could potentially have multiple impacts on disease outcome, including presenting challenges to therapeutics. First, we found that vacuolar bound bacteria were more tolerant to a cell-permeable antibiotic than their cytosolic counterparts. Persistence and antibiotic recalcitrance of vacuole-contained bacteria could be a contributor to why *P. aeruginosa* infections are difficult to treat and why infection can rebound after antibiotic treatment is ended. Second, the data showed that the vacuolar population triggered lytic host cell death contingent on their viability, even when the cytosolic population is eliminated using an antibiotic. Indeed, use of an antibiotic at concentrations killing only the cytosolic population actually promotes this type of cell death because the cytosolic population uses ExoS to counter it (16). Since lytic cell death releases inflammatory mediators, its inhibition by ExoS likely serves to limit host responses to infection while also preserving the replicative niche. If so, killing cytosolic bacteria with antibiotics that preserve the vacuolar population could favor immune responses/inflammation. How this would play out in an actual infection (e.g., increased bacterial clearance versus damaging inflammation) will require further investigation given the complexities of *in vivo* systems. An additional consideration relates to the design of novel therapies (e.g., targeting bacterial biofilms) if they need to access an intracellular niche enclosed by two host membrane layers.

Intravital confocal imaging of infected mouse corneas was used to explore the location of *P. aeruginosa* within cells after *in vivo* infection. The methods used allowed spatial and temporal resolution and, therefore, accurate localization of bacteria with respect to cell membranes over time in addition to their depth within the tissue. Bacteria were detected in the cytosol of infected epithelial cells, some deep within the tissue and others closer to the corneal surface. As we have shown *in vitro*, this included multiple bacteria disseminating through the cell cytoplasm at speeds/pattern aligning with twitching motility, with some cells (also or instead) containing rapidly swimming bacteria inside membrane blebs. A third intracellular bacterial population was detected resembling *P. aeruginosa*-containing vacuoles occurring in cultured epithelial cells. While the fluorescent signal from bacteria packed inside vacuoles merges to prevent resolution of individual bacteria, the circular shape of the emanating fluorescence implies that these bacterium-containing regions are surrounded by a vacuolar membrane.

Mutants lacking the T3SS (Δ*exsA*) remain in vacuoles because they lack the ability

to escape the vacuole. These were also found to express biofilm-associated factors, essentially phenocopying T3SS-negative subpopulations of the wild type persisting in vacuoles. While showing that T3SS mutants can be used to study the phenotype, this result also suggests that lack of T3SS expression and, subsequently, the vacuolar environment may drive biofilm production. Biofilm production in response to the vacuolar environment aligns with our current understanding of biofilms, which can help bacteria tolerate adverse environmental conditions such as nutrient limitation, host immune responses, and exposure to antibiotics (3, 4, 27, 31, 51, 52) and is therefore triggered by such conditions. There are many aspects of the vacuole environment with the potential to trigger the production of biofilm, including vacuolar acidification and expression of intracellular antimicrobial factors such as defensin antimicrobial peptides, reactive oxygen species, and lytic enzymes, which all form part of the antimicrobial activity of phagolysosomes (53). Alternatively, biofilm production in vacuoles might relate to the T3SS-off state. *P. aeruginosa* can switch back and forth between the T3SS-on/motile/rapid growth state and a T3SS-off/non-motile/biofilm-producing/slow growth/antibiotic-tolerant state, which is controlled by a complex regulatory system (Gac/Rsm pathway) (54). This is often referred to as the acute/chronic switch in infection because the former supports acute infection pathogenesis and the latter promotes persistence and chronic infection. While features of the cytosolic versus vacuolar niches arising when *P. aeruginosa* diversifies inside cells are reminiscent of the acute and chronic states, the latter are generally believed to occur in different infection types, or at least different time points during infection. Here, we have found that the intracellular phenotypes occur simultaneously (including in the same cell), and they both occur relatively early (acute T3SS^{on} 4 h and *cdrA*^{on} 6 h). Related to this, others have reported other situations when the lines between acute and chronic infection phenotypes are blurred (55, 56). More work will be needed to understand the relationship, if any, between intracellular diversity of *P. aeruginosa* and previously described phenotypic switches.

Our data showed that *P. aeruginosa* in vacuoles expressed biofilm factors known to help it persist in the host and other adverse environments. They were also more antibiotic-tolerant than *P. aeruginosa* found elsewhere in the cell, which did not express biofilm factors. Nevertheless, mutants lacking the biofilm protein CdrA and all three biofilm-associated exopolysaccharides retained their ability to persist in vacuoles and tolerate antibiotics, showing that these factors were not required. Accordingly, only a subfraction of the vacuolar population expressed *cdrA* when the wild type was used, and the total percentage of cells containing antibiotic-tolerant bacteria exceeded the fraction expressing *cdrA*. While inconsistent *cdrA* expression might relate to different stages of maturation in the vacuole, this result provides further evidence that *cdrA* is not required.

Possible explanations for these results include functional redundancy with other biofilm-associated factors or that different biofilm-associated factors are responsible—possibly even novel biofilm factors produced in this location. Alternatively, persistence/antibiotic tolerance might not be due to biofilm factors. Other possibilities include a reduced growth rate, which can decrease sensitivity to fluoroquinolones (52). Division rates for vacuolar bacteria were obviously slower than the rapid replication occurring in the cytosol (Fig. 3A and D and Fig. 5A), which is not surprising given space and nutrient limitations and other adverse conditions expected in vacuoles. Other phenotypic changes that could participate include expression of multidrug efflux pumps or factors that modulate cell wall permeability (57–59) or the fact that vacuolar bacterial subpopulation(s) enter a persister state in the face of ofloxacin exposure (60). Rather than being a property of the enclosed bacteria, enhanced tolerance in vacuoles might instead relate to vacuolar properties. While the antibiotic is cell permeable, there will still be some exclusion by the vacuolar membrane. In this regard, the concentration needed to kill cytosolic bacteria (enclosed by the host cell plasma membrane) was somewhat higher than that needed to kill extracellular bacteria (~2-fold). This alone is unlikely to explain the ~4- to 8-fold additional tolerance of vacuolar bacteria on the other side of

a second membrane. However, it is possible that *P. aeruginosa*, like other intracellular vacuolar bacteria, modifies the vacuolar membrane (46, 47, 61, 62). Whether such modification to the vacuolar membrane limits penetration of antibiotics remains unknown. Since there are many possibilities, pinpointing the mechanisms by which *P. aeruginosa* persists in vacuoles will require further investigation, which could lead to novel strategies for treating antibiotic-recalcitrant infections.

While studying the exopolysaccharide (EPS) mutants, we found that they persisted in cells even more efficiently than the wild type, the results showing that they occupied ~25 to 30% of cells versus ~15 to 20% of cells for the wild type or *cdrA* mutants able to express EPS (Fig. 6C and D, gray bars). Interestingly, initial internalization (at 4 h) of the wild type and Δ*EPS* mutants was similar (Fig. S2), suggesting that greater intracellular persistence of Δ*EPS* mutants at 12 h (Fig. 6C and D) was not due to loss of antiphagocytic activity, the latter being a well-established role for exopolysaccharides in other types of bacteria. However, determining how EPS contributes to modification of bacterial persistence was beyond the scope of our aims.

This study further demonstrates the advantage of time-lapse imaging for studying intracellular bacterial populations, particularly for those with a complex lifestyle. For instance, the detection and quantification of fluorescent bacteria using gene-expression reporters allowed the delineation of viable intracellular subpopulations in real time. Moreover, this methodology is especially of value when studying bacterial persistence after antibiotic treatment, as it can detect metabolically active bacteria that may not be quantifiable using traditional CFU counting, e.g., viable but nonculturable cells. Another advantage of imaging, labeling cellular structures, use of high-resolution methods, and including temporal information is being able to distinguish intracellular bacteria from antibiotic-recalcitrant extracellular bacteria, which can occur if bacteria form extracellular biofilms around the cells being studied (63, 64). A potential caveat of our study relates to the arabinose-inducible GFP expression method we used to visualize all intracellular bacteria irrespective of gene expression profile. Recent studies have shown that with some promoters, including the one used here, expression can be impacted by Vfr (65, 66), in which case the number of intracellular bacteria might be greater than those we detected using this method.

In conclusion, this study furthers our understanding of the intracellular lifestyle of *P. aeruginosa* by demonstrating that it diversifies intracellularly to form viable subpopulations in both vacuoles and the cytoplasm of epithelial cells. In these distinct locations they adopt different phenotypes and functions. T3SS-expressing bacteria exit vacuoles, disseminate through the cytoplasm using twitching motility, and use ExoS to replicate rapidly, avoid autophagy, and inhibit cell death to keep the replicative niche alive. Some of these T3SS-expressing cytosolic bacteria also use ExoS to assemble and occupy membrane bleb niches that can subsequently detach, allowing vesicle-contained T3SS-expressing bacteria to travel to distant locations (9). Meanwhile, vacuolar populations in the same or adjacent cells grow slowly, express biofilm-associated factors, tolerate antibiotics, and in the absence of cytosolic cell-mates trigger death of the infected host cell. Since the different phenotypes can occur in the same cell, cooperation is likely and might ensure that both short- and long-term interests are met. Other bacteria able to adopt an intracellular lifestyle tend to establish one type of niche in an infected cell type, even if they traffic through various compartments to arrive there. The unique ability of *P. aeruginosa* to diversify intracellularly and assemble multiple niches associated with differential gene expression is likely to contribute to the reasons why it is a highly effective opportunistic pathogen and why infections caused by it are so difficult to treat.

MATERIALS AND METHODS

Cell culture. Human corneal epithelial cells (hTCEpi) (67) were cultured in KGM-2 (Lonza, USA) supplemented with 1.15 mM calcium chloride (high calcium) to allow differentiation and were maintained at 37°C (humidified) in a 5% CO_2 incubator. Human bronchial epithelial cells (NuLi-1) were cultured as previously described (19) in bronchial epithelial cell growth medium (BEGM) (Lonza, USA) with 1.15 mM calcium chloride and maintained as for hTCEpi. Epithelial cells were grown as monolayers on 24-well tissue culture dishes (MatTek Corporation, Ashland, MA) for wide-field microscopy or plasmid

TABLE 2 Primers used in this study

ID	Primer name	Sequence (5′–3′)	Restriction site	Expected size
P019	pJNE05_part1.1a	ACCTTCGGGAGCGCCTGA		3,106 bp
P020	pJNE05_part1.1b	agtactattgaacgcgtGAATTCGGCTTATTCCCTAAC		
P021	pJNE05_part2.1a	ttagggaataagccgaattcacgcgttcaatagtactAAGCTTCCGATCCCCAATTCC		3,486 bp
P022	pJNE05_part2.1b	cttcaggcgctcccgaaggtCTCGGGCCGTCTCTTGGG		
P032	cdrA.1a	cactaagtactCATTGTCGGTTTTTTGACGG		
P033	cdrA.1b	cactaacgcgtCGCACGTCAGTTTTCCAGCA		
P010	ptac-dTomato.1a	TTATAggcgcgcctgcaggtcgtaaatcactgc	AscI site	419 bp plus dTomato ~1 kb
P011	ptac-dTomato.1b	TATTAgcggccgccttctctcatccgccaaaac	NotI site	
P014	T0T1-terminators.1a	atgagagaagggcgcgccAGCTTAATTAGCTGAGCTTGG	AscI site mid-primer	300 bp
P015	T0T1-terminators.1b	cctattctctagaactagtgCGGCGGATTTGTCCTACTC		
P027	ebfp2.1a	cactaggatccAATGGTGAGCAAGGGCGAGG	BamHI site	746 bp
P029	ebfp2.2b	CACATAAGCTTCTTACTTGTACAGCTCGTCCATGCC	HindIII site	
P012	pMG035-gibson.1a	taccgggccccccctcgaggtcgacTGCAGGTCGTAAATCACTG	SalI site mid-primer	1,075 bp
P013	pMG035-gibson.1b	ttaagctggcgcgccCTTCTCTCATCCGCCAAAAC	AscI site mid-primer	

validation or on 8-well tissue culture dishes (ibidi, Gräfelfing, Germany) or glass-coverslips for use in immunofluorescence.

Bacterial strains, plasmids, and mutants. *P. aeruginosa* strains and plasmids are shown in Table 1. Bacteria were grown at 37°C on Trypticase soy agar (TSA) (Hardy Diagnostics, Santa Maria, CA) for 16 h before use. For imaging, bacteria were transformed with either the T3SS-GFP reporter (pJNE05), c-di-GMP Turbo-RFP reporter (pFy4535) (39), *cdrA*-GFP reporter (pMG078), or pBAD-GFP (arabinose-inducible, $pGFP_{arabinose}$) and grown on media supplemented with gentamicin (100 μg/mL). Bacterial inocula were prepared by resuspending bacterial colonies into sterile phosphate-buffered saline (PBS) to an optical density (OD) at 550 nm of 1.0 (~2×10^8 CFU/mL).

To construct plasmid pMG078 (*cdrA*-GFP), the pJNE05 empty vector was engineered to have a promoter-less *gfp* and MluI and ScaI restriction sites were added upstream of the *gfp* to create a multiple cloning site for introducing any promoter of interest. Briefly, pJNE05 was prepared as two large PCR products with overlapping ends, with the MluI and ScaI sites added to the primers and excluding the promoter already present in the native pJNE05 vector. Fragment 1 was amplified using the primer pair with engineered restriction sites indicated in bold. pJNE05_part1.1a and pJNE05_part1.1b- and fragment 2 were amplified using pJNE05_part2.1a and pJNE05_part2.1b (Table 2). The two fragments with overlapping ends were assembled by Gibson assembly. The *cdrA* promoter region for the promoter-*gfp* fusion was then amplified using previously published primers (68) with slight modification for our vector backbone (cdrA.1a and cdrA.1b, Table 2). The resulting fragment and promoter-less *gfp*-pJNE05 backbone were digested with MluI and ScaI and then fused by T4 DNA ligase to construct the pMG078 vector. The prepared *cdrA*-GFP fusion reporter was confirmed by the comparing relative fluorescence intensity in the wild type (WT) (PAO1F) and the PAO1FΔ*fleQ* mutant (11) in the stationary phase of batch culture after ~12 h growth in TSB at 37°C (normalized to OD at 650 nm) (Fig. S1A). Sensitivity of the *cdrA*-GFP reporter (pMG078) to high levels of c-di-GMP was determined by comparing the relative fluorescence intensity in the WT (PAO1P; low c-di-GMP) and the mutant PAO1PΔ*wspF* (hi-c-di-GMP) over 24 h of growth in TSB at 37°C in a Biotek plate reader at 200 rpm recording every 30 min (Fig. S1B).

To construct pBAD-GFP ($pGFP_{arabinose}$), the promoter region of the pJNE05 was replaced with an arabinose-inducible promoter region. The *exoS* promoter of pJNE05 was excised by digestion with HindIII and EcoRI and replaced with the arabinose-inducible promoter from plasmid pTJ1. Validation of $pGFP_{arabinose}$ *in vitro* was performed using hTCEpi cultured on 24-well plates. Epithelial cells were inoculated with PAO1F::$pGFP_{arabinose}$ or PAO1FΔ*exsA*::$pGFP_{arabinose}$ (~2×10^6 CFU bacteria, MOI of 10) for 3 h. Extracellular bacteria were killed by adding amikacin (200 μg/mL) for 30 min. GFP expression was induced after 30 min by adding medium containing 1% L-arabinose, and the GFP signal was recorded hourly for 8 h on a Nikon Ti Eclipse inverted wide-field microscope (Fig. S1).

Plasmid pMG055 (constitutive blue fluorescent protein, EBFP2) was constructed as follows. Briefly, to start, pMG046 was generated by cloning the tac promoter and dTomato from p67T1 (69) and was cloned into the AscI/NotI site of pTJ1. *Ebfp2* from the plasmid pBAD-*ebfp*2 (purchased from Addgene) was then cloned into the BamHI/HindIII site of pMG046 downstream of the tac promoter (replacing dTomato) to create pMG051. Then, the ptac-*ebfp2* construct was amplified from pMG051, plus the T0T1 terminator fragment amplified from pTJ1, and cloned via Gibson assembly into the SalI/BamHI site of a promoter-less GFP pJNE05-based plasmid to yield pMG055, which has a constitutive EBFP2, and a promoter-less *gfp* gene.

Bacterial internalization assays. Epithelial cells were inoculated with 5 μL (containing ~2×10^6 CFU bacteria) of a suspension of *P. aeruginosa* PAO1 wild type or mutants transformed with fluorescent reporter plasmids (MOI, 10) and incubated for 3 h at 37°C (internalization period). Epithelial cells were then incubated with cell culture medium (KGM-2 or BEGM plus 1.15 mM calcium) supplemented with amikacin (200 μg/mL) for 1 h to kill extracellular bacteria. To explore the ofloxacin susceptibility of intracellular bacteria, epithelial cells were exposed to both amikacin (200 μg/mL) and ofloxacin at concentrations ranging from the MIC to

16× MIC. Controls were treated with cell culture medium including matched levels of acetic acid diluent. In some experiments, $pGFP_{arabinose}$ was activated 30 min after extracellular antibiotic was administered using 1% L-arabinose.

Microscopy. Live and time-lapse images were captured on a Nikon Ti-E inverted wide-field fluorescence microscope equipped with a Lumencor Spectra X illumination source and an Okolab Uno-combined controller stage top incubation chamber to maintain heat, humidity, and 5% CO_2. Time-lapse images were captured using a CFI Plan Apochromat Lambda 40× air objective equipped with differential interference contrast (DIC). Live phase-contrast images were captured using a Plan Apochromat Lambda Ph3DM 60× oil-immersion objective. For time-lapse imaging, fields were chosen visualizing DIC only to identify areas free of debris; TurboRFP and GFP were not observed until the time-lapse imaging was completed to avoid bias in field selection. For time-lapse imaging with quantification, eight fields were imaged for each condition. For live phase-contrast without quantification, three fields were imaged for each condition.

Ofloxacin stock solutions and determination of MIC. Target ofloxacin concentrations from 0.0625 to 8 μg/mL were obtained by dilution of a 10- mg/mL stock solution (prepared in 100% acetic acid) in cell culture medium. Concentrations of 16 to 64 μg/mL were prepared by diluting a 6.4-mg/mL stock solution (prepared in 10% acetic acid) by 1:400 to 1:100. Similarly, a concentration of 25 μg/mL was prepared by diluting a 2.5-mg/mL stock solution (prepared in 10% acetic acid) by 1:100 dilution. Dilutions were such that acetic acid levels in each assay were below 0.1%. The MIC of ofloxacin against *P. aeruginosa* wild-type and mutant strains was determined by inoculating $\sim 1.5 \times 10^8$ CFU of bacteria in tryptic soy broth into a 96-well plate at 37°C and then incubating the plate overnight (16 h) in the presence of ofloxacin at the above-mentioned concentrations. The MIC was determined as the lowest concentration that inhibited bacterial growth measured by absorbance at 550 nm.

Immunofluorescence. Epithelial cells were cultured and inoculated with bacteria as described above. After 3 h, KGM-2 (plus 1.15 mM calcium) containing amikacin (200 μg/mL) was added to kill extracellular bacteria for 3 h at 37°C or amikacin with ofloxacin (up to 16× MIC) added to also challenge intracellular bacteria. At 6 h postinoculation, cells were washed with PBS and fixed in fresh 4% paraformaldehyde (PFA) (Sigma-Aldrich) for 10 min. After an additional PBS wash, cells were permeabilized for 10 min using 4% PFA containing 0.1% Triton X-100. Cells were quenched with aldehydes in 150 mM glycine (Sigma-Aldrich) for 10 min, washed in PBS, and blocked for 1 h at room temperature in 0.7% fish skin gelatin (Sigma-Aldrich). All *P. aeruginosa* bacteria were labeled with anti-*Pseudomonas* antibody (Abcam, no. ab74980, primary) with Alexa-Fluor 555 (Sigma, secondary) for 1 h. For all preparations, cells were washed with PBS; ProLong Diamond antifade mounting medium (Thermo Fisher Scientific) was applied, and samples were sealed with a coverslip and imaged. Epithelial cell nuclei were stained with NucBlue Live ReadyProbes reagent (Thermo Fisher Scientific).

Correlative light-electron microscopy (CLEM). The hTCEpi were grown to 70% confluence on 35-mm gridded MatTek dishes with a glass bottom by adding $\sim 6 \times 10^5$ cells in KGM-2 medium containing 1.15 mM calcium chloride and incubation overnight in a cell culture incubator. Prior to infection, Hoechst dye was added at a concentration of 3 μL/mL to stain the nuclei. Epithelial cells were infected with bacteria at an MOI of 10 and allowed to progress for 3 h. At this time, a 1:1 dilution of prewarmed amikacin (400 μg/mL) in KGM-2 plus 1.15 mM calcium was added for 30 min, followed by ofloxacin to a final concentration of 1 μg/mL for 3 h (total infection time, 6 h). At 6 h, 2 mL of medium was removed, leaving 1 mL behind to prevent cells from drying. Cells were washed three times with the sequential addition of 1 mL of cell culture medium, always leaving behind 1 mL. Cells were fixed with 1 mL of fixative medium in KGM-2 (8% electron microscopy-grade paraformaldehyde [PFA]) for a minimum of 30 min. All fluorescent images were obtained in PFA-containing medium. Following fluorescence imaging, cells were fixed in 2.5% glutaraldehyde and 2.5% paraformaldehyde in 0.1 M sodium cacodylate buffer, pH 7.4 (EMS, Hatfield, PA, USA). Samples were rinsed 3 times (5 min each) at room temperature in 0.1 M sodium cacodylate buffer, pH 7.2, and immersed in 1% osmium tetroxide with 1.6% potassium ferricyanide in 0.1 M sodium cacodylate buffer for 30 min. Samples were rinsed 3 times (5 min each) at room temperature in buffer and briefly washed once with distilled water (1 min) at room temperature. Samples were then subjected to an ascending ethanol gradient followed by pure ethanol. Samples were then progressively infiltrated (using ethanol as the solvent) with Epon resin (EMS) and polymerized at 60°C for 24 to 48 h. Care was taken to ensure that only a thin amount of resin remained within the glass-bottom dishes to enable the best possible chance for separation of the glass coverslip. Following polymerization, the glass coverslips were removed using ultrathin Personna razor blades (EMS) and liquid nitrogen exposure, as needed. Correlative light-electron microscopy (CLEM), was performed to visualize specific cells of interest. Regions of interest, identified by the gridded alpha-numerical labeling on the plates, were carefully removed, precisely trimmed to the cell of interest, and mounted on a blank resin block with cyanoacrylate glue for sectioning. Serial thin sections (80 nm) were cut using a UC6 ultramicrotome (Leica, Wetzlar, Germany) from the surface of the block until approximately 4 to 5 microns within to ensure complete capture of the cell volumes. Section-ribbons were then collected sequentially onto Formvar-coated slot- or 50-mesh grids. The grids were poststained with 2% uranyl acetate followed by Reynold's lead citrate for 5 min each. Sections were imaged using a Tecnai 12 120 kV TEM (FEI, Hillsboro, OR, USA), and data were recorded using either a Gatan US1000 CCD with Digital Micrograph 3 or a Gatan Rio 16 CMOS with Gatan Microscopy Suite software (Gatan, Inc., Pleasanton, CA, USA).

Murine infection model. All procedures involving animals were carried out in accordance with the standards established by the Association for the Research in Vision and Ophthalmology, under protocol AUP-2019-06-12322, approved by the Animal Care and Use Committee, University of California Berkeley. This protocol adheres to PHS policy on the humane care and use of laboratory animals and the guide for the care and use of laboratory animals. For *in vivo* imaging of corneal infection by *P. aeruginosa*, 8- to

10-week-old female C57BL/6 Lyz2cre+/mRosa-DTR mice (F1 cross) were used since they express red fluorescent membranes and green/yellow myeloid-derived cells. The cornea scarification model was used to establish infection as previously described (70, 71). Briefly, mice were anesthetized for 4 h by ketamine-dexmedetomidine injection (ketamine, 80-100mg/Kg; dexmedetomidine, 0.25 to 0.5 mg/Kg), and the cornea of one eye was scratched in parallel three times with a sterile 26 G needle and then inoculated with 5 μL of wild-type mPAO1-EBF2 (pMG055; constitutive blue fluorescent protein) in suspension containing $\sim 10^9$ CFU of bacteria at 1-h intervals for 4 h while under continued ketamine-dexmedetomidine anesthesia. After 4 h, mice were woken up with anesthesia reversal agent Atipamezole via injection (2.5 to 5 mg/Kg) and remained under supervision for 10 h. At 15 h, mice were reanesthetized with ketamine-dexmedetomidine injection (ketamine, 80-100mg/Kg; dexmedetomidine, 0.25 to 0.5 mg/Kg), and the infected corneas were imaged in the live animals by confocal microscopy.

Statistical analysis. Prism software was used for numerical data analysis. Data were expressed as a mean ± standard deviation (SD). Two-group comparisons were performed using Student's *t* test, and multiple-group analysis was performed using one-way analysis of variance (ANOVA) with Dunnett's multiple-comparison test. *P* values less than 0.05 were considered significant.

SUPPLEMENTAL MATERIAL

Supplemental material is available online only.

VIDEO S1, MOV file, 1.8 MB.
VIDEO S2, MOV file, 1.8 MB.
VIDEO S3, MOV file, 1.8 MB.
VIDEO S4, MOV file, 0.6 MB.
VIDEO S5, MOV file, 0.02 MB.
VIDEO S6, MOV file, 0.02 MB.
FIG S1, TIF file, 0.75 MB.
FIG S2, TIF file, 0.24 MB.

ACKNOWLEDGMENTS

Thanks to Alain Filloux (Imperial College London, UK), Fitnat Yildiz (University of California Santa Cruz, CA), and Matthew Parsek (University of Washington, WA) for providing *P. aeruginosa* wild-type strains, mutants, and plasmid constructs. Thanks to Danielle Robertson (University of Texas Southwestern, TX) for providing the telomerase-immortalized human corneal epithelial cells. Thanks to Danielle Jorgens and Reena Zalpuri at the University of California Berkeley Electron Microscope Laboratory for expert advice and assistance with electron microscopy.

N.G.K., V.N., A.R.K., M.R.G., M.M.E.M., T.L.Y., D.J.E., and S.M.J.F. designed the experiments; N.G.K., V.N., A.R.K., E.J., M.E.H., M.R.G., and M.M.E.M. performed the experiments; N.G.K., V.N., A.R.K., M.R.G., M.M.E.M., T.L.Y., D.J.E., and S.M.J.F. analyzed and interpreted the data; N.G.K., V.N., A.R.K., D.J.E., and S.M.J.F. wrote the manuscript; D.J.E. and S.M.J.F. supervised the study.

This work was supported by the National Institutes of Health R01 EY011221 (S.M.J.F.), F32 EY029152 (V.N.), and F32 EY025969 (A.R.K.); by the Elizabeth Nash Memorial Fellowship awarded by the Cystic Fibrosis Research Institute (N.G.K.), and by the American Heart Association (M.R.G.). The funding agencies had no role in the study design, data collection and interpretation, or decision to submit the work for publication.

REFERENCES

1. Sader HS, Huband MD, Castanheira M, Flamm RK. 2017. *Pseudomonas aeruginosa* antimicrobial susceptibility results from four years (2012 to 2015) of the International Network for Optimal Resistance Monitoring Program in the United States. Antimicrob Agents Chemother 61:e02252-16. https://doi.org/10.1128/AAC.02252-16.
2. Mulcahy LR, Isabella VM, Lewis K. 2014. *Pseudomonas aeruginosa* biofilms in disease. Microb Ecol 68:1–12. https://doi.org/10.1007/s00248-013-0297-x.
3. Moradali MF, Ghods S, Rehm BHA. 2017. *Pseudomonas aeruginosa* lifestyle: a paradigm for adaptation, survival, and persistence. Front Cell Infect Microbiol 7:39.
4. Winstanley C, O'Brien S, Brockhurst MA. 2016. *Pseudomonas aeruginosa* evolutionary adaptation and diversification in cystic fibrosis chronic lung infections. Trends Microbiol 24:327–337. https://doi.org/10.1016/j.tim.2016.01.008.
5. Fleiszig SMJ, Kroken AR, Nieto V, Grosser MR, Wan SJ, Metruccio MME, Evans DJ. 2020. Contact lens-related corneal infection: Intrinsic resistance and its compromise. Prog Retin Eye Res 76:100804. https://doi.org/10.1016/j.preteyeres.2019.100804.
6. Fleiszig SM, Zaidi TS, Fletcher EL, Preston MJ, Pier GB. 1994. *Pseudomonas aeruginosa* invades corneal epithelial cells during experimental infection. Infect Immun 62:3485–3493. https://doi.org/10.1128/iai.62.8.3485-3493.1994.
7. Fleiszig SM, Zaidi TS, Pier GB. 1995. *Pseudomonas aeruginosa* invasion of and multiplication within corneal epithelial cells *in vitro*. Infect Immun 63:4072–4077. https://doi.org/10.1128/iai.63.10.4072-4077.1995.
8. Fleiszig SMJ, Zaidi TS, Preston MJ, Grout M, Evans DJ, Pier GB. 1996. Relationship between cytotoxicity and corneal epithelial cell invasion by

clinical isolates of *Pseudomonas aeruginosa*. Infect Immun 64:2288–2294. https://doi.org/10.1128/iai.64.6.2288-2294.1996.
9. Angus AA, Lee AA, Augustin DK, Lee EJ, Evans DJ, Fleiszig SMJ. 2008. *Pseudomonas aeruginosa* induces membrane blebs in epithelial cells, which are utilized as a niche for intracellular replication and motility. Infect Immun 76:1992–2001. https://doi.org/10.1128/IAI.01221-07.
10. Heimer SR, Evans DJ, Stern ME, Barbieri JT, Yahr T, Fleiszig SMJ. 2013. *Pseudomonas aeruginosa* utilizes the type III secreted toxin ExoS to avoid acidified compartments within epithelial cells. PLoS One 8:e73111. https://doi.org/10.1371/journal.pone.0073111.
11. Kroken AR, Chen CK, Evans DJ, Yahr TL, Fleiszig SMJJ. 2018. The Impact of ExoS on *Pseudomonas aeruginosa* Internalization by epithelial cells is independent of *fleQ* and correlates with bistability of type three secretion system gene expression. mBio 9:e00668-18. https://doi.org/10.1128/mBio.00668-18.
12. Sana TG, Baumann C, Merdes A, Soscia C, Rattei T, Hachani A, Jones C, Bennett KL, Filloux A, Superti-Furga G, Voulhoux R, Bleves S. 2015. Internalization of *Pseudomonas aeruginosa* strain PAO1 into epithelial cells is promoted by interaction of a T6SS effector with the microtubule network. mBio 6:e00712-15. https://doi.org/10.1128/mBio.00712-15.
13. Fleiszig SM, Wiener-Kronish JP, Miyazaki H, Vallas V, Mostov KE, Kanada D, Sawa T, Yen TS, Frank DW. 1997. *Pseudomonas aeruginosa*-mediated cytotoxicity and invasion correlate with distinct genotypes at the loci encoding exoenzyme S. Infect Immun 65:579–586. https://doi.org/10.1128/iai.65.2.579-586.1997.
14. Zaidi TS, Fleiszig SM, Preston MJ, Goldberg JB, Pier GB. 1996. Lipopolysaccharide outer core is a ligand for corneal cell binding and ingestion of *Pseudomonas aeruginosa*. Invest Ophthalmol Vis Sci 37:976–986.
15. Hritonenko V, Evans DJJ, Fleiszig SMJM. 2012. Translocon-independent intracellular replication by *Pseudomonas aeruginosa* requires the ADP-ribosylation domain of ExoS. Microbes Infect 14:1366–1373. https://doi.org/10.1016/j.micinf.2012.08.007.
16. Kroken AR, Gajenthra Kumar N, Yahr TL, Smith BE, Nieto V, Horneman H, Evans DJ, Fleiszig SMJ. 2022. Exotoxin S secreted by internalized *Pseudomonas aeruginosa* delays lytic host cell death. PLoS Pathog 18:e1010306. https://doi.org/10.1371/journal.ppat.1010306.
17. Angus AA, Evans DJ, Barbieri JT, Fleiszig SMJ. 2010. The ADP-ribosylation domain of *Pseudomonas aeruginosa* ExoS is required for membrane bleb niche formation and bacterial survival within epithelial cells. Infect Immun 78:4500–4510. https://doi.org/10.1128/IAI.00417-10.
18. Cowell BA, Chen DY, Frank DW, Vallis AJ, Fleiszig SMJ. 2000. ExoT of cytotoxic *Pseudomonas aeruginosa* prevents uptake by corneal epithelial cells. Infect Immun 68:403–406. https://doi.org/10.1128/IAI.68.1.403-406.2000.
19. Jolly AL, Takawira D, Oke OO, Whiteside SA, Chang SW, Wen ER, Quach K, Evans DJ, Fleiszig SMJ. 2015. *Pseudomonas aeruginosa*-induced bleb-niche formation in epithelial cells is independent of actinomyosin contraction and enhanced by loss of cystic fibrosis transmembrane-conductance regulator osmoregulatory function. mBio 6:e02533. https://doi.org/10.1128/mBio.02533-14.
20. Evans DJ, Frank DW, Finck-Barbançon V, Wu C, Fleiszig SMJ. 1998. *Pseudomonas aeruginosa* invasion and cytotoxicity are independent events, both of which involve protein tyrosine kinase activity. Infect Immun 66:1453–1459. https://doi.org/10.1128/IAI.66.4.1453-1459.1998.
21. Diaz MR, King JM, Yahr TL. 2011. Intrinsic and extrinsic regulation of type III secretion gene expression in *Pseudomonas aeruginosa*. Front Microbiol 2:89. https://doi.org/10.3389/fmicb.2011.00089.
22. Garai P, Berry L, Moussouni M, Bleves S, Blanc-Potard A-B. 2019. Killing from the inside: Intracellular role of T3SS in the fate of *Pseudomonas aeruginosa* within macrophages revealed by *mgtC* and *oprF* mutants. PLoS Pathog 15:e1007812. https://doi.org/10.1371/journal.ppat.1007812.
23. Rao L, De La Rosa I, Xu Y, Sha Y, Bhattacharya A, Holtzman MJ, Gilbert BE, Eissa NT. 2021. *Pseudomonas aeruginosa* survives in epithelia by ExoS-mediated inhibition of autophagy and mTOR. EMBO Rep 22:1–15. https://doi.org/10.15252/embr.202050613.
24. Goldberg MB. 2001. Actin-based motility of intracellular microbial pathogens. Microbiol Mol Biol Rev 65:595–626. https://doi.org/10.1128/MMBR.65.4.595-626.2001.
25. Nieto V, Kroken AR, Grosser MR, Smith BE, Metruccio MME, Hagan P, Hallsten ME, Evans DJ, Fleiszig SMJ. 2019. Type IV pili can mediate bacterial motility within epithelial cells. mBio 10:e02880-18. https://doi.org/10.1128/mBio.02880-18.
26. López D, Vlamakis H, Kolter R. 2010. Biofilms. Cold Spring Harb Perspect Biol 2:a000398. https://doi.org/10.1101/cshperspect.a000398.
27. Donlan RM, Costerton JW. 2002. Biofilms: survival mechanisms of clinically relevant microorganisms. Clin Microbiol Rev 15:167–193. https://doi.org/10.1128/CMR.15.2.167-193.2002.
28. Lyczak JB, Cannon CL, Pier GB. 2002. Lung infections associated with cystic fibrosis. Clin Microbiol Rev 15:194–222. https://doi.org/10.1128/CMR.15.2.194-222.2002.
29. Drenkard E, Ausubel FM. 2002. *Pseudomonas* biofilm formation and antibiotic resistance are linked to phenotypic variation. Nature 416:740–743. https://doi.org/10.1038/416740a.
30. Wagner VE, Iglewski BH. 2008. *P. aeruginosa* biofilms in CF infection. Clin Rev Allergy Immunol 35:124–134. https://doi.org/10.1007/s12016-008-8079-9.
31. Whiteley M, Bangera MG, Bumgarner RE, Parsek MR, Teitzel GM, Lory S, Greenberg EP. 2001. Gene expression in *Pseudomonas aeruginosa* biofilms. Nature 413:860–864. https://doi.org/10.1038/35101627.
32. Colvin KM, Irie Y, Tart CS, Urbano R, Whitney JC, Ryder C, Howell PL, Wozniak DJ, Parsek MR. 2012. The Pel and Psl polysaccharides provide *Pseudomonas aeruginosa* structural redundancy within the biofilm matrix. Environ Microbiol 14:1913–1928. https://doi.org/10.1111/j.1462-2920.2011.02657.x.
33. Ryder C, Byrd M, Wozniak DJ. 2007. Role of polysaccharides in *Pseudomonas aeruginosa* biofilm development. Curr Opin Microbiol 10:644–648. https://doi.org/10.1016/j.mib.2007.09.010.
34. Borlee BR, Goldman AD, Murakami K, Samudrala R, Wozniak DJ, Parsek MR. 2010. *Pseudomonas aeruginosa* uses a cyclic-di-GMP-regulated adhesin to reinforce the biofilm extracellular matrix. Mol Microbiol 75:827–842. https://doi.org/10.1111/j.1365-2958.2009.06991.x.
35. Reichhardt C, Wong C, da Silva DP, Wozniak DJ, Parsek MR. 2018. CDRA interactions within the *Pseudomonas aeruginosa* biofilm matrix safeguard it from proteolysis and promote cellular packing. mBio 9:e01376-18. https://doi.org/10.1128/mBio.01376-18.
36. Jennings LK, Storek KM, Ledvina HE, Coulon C, Marmont LS, Sadovskaya I, Secor PR, Tseng BS, Scian M, Filloux A, Wozniak DJ, Howell PL, Parsek MR. 2015. Pel is a cationic exopolysaccharide that cross-links extracellular DNA in the *Pseudomonas aeruginosa* biofilm matrix. Proc Natl Acad Sci U S A 112:11353–11358. https://doi.org/10.1073/pnas.1503058112.
37. Okshevsky M, Meyer RL. 2015. The role of extracellular DNA in the establishment, maintenance and perpetuation of bacterial biofilms. Crit Rev Microbiol 41:341–352. https://doi.org/10.3109/1040841X.2013.841639.
38. Cherny KE, Sauer K. 2020. Untethering and degradation of the polysaccharide matrix are essential steps in the dispersion response of *Pseudomonas aeruginosa* biofilms. J Bacteriol 202:e00575-19. https://doi.org/10.1128/JB.00575-19.
39. Zamorano-Sánchez D, Xian W, Lee CK, Salinas M, Thongsomboon W, Cegelski L, Wong GCL, Yildiz FH. 2019. Functional specialization in *Vibrio cholerae* diguanylate. mBio 10:1–16. https://doi.org/10.1128/mBio.00670-19.
40. Zhou H, Zheng C, Su J, Chen B, Fu Y, Xie Y, Tang Q, Chou SH, He J. 2016. Characterization of a natural triple-tandem c-di-GMP riboswitch and application of the riboswitch-based dual-fluorescence reporter. Sci Rep 6:20871. https://doi.org/10.1038/srep20871.
41. Reichhardt C, Jacobs HM, Matwichuk M, Wong C, Wozniak DJ, Parsek MR. 2020. The versatile *Pseudomonas aeruginosa* biofilm matrix protein CdrA promotes aggregation through different extracellular exopolysaccharide interactions. J Bacteriol 202:1–9. https://doi.org/10.1128/JB.00216-20.
42. Hsiao JY, Chen CY, Yang MJ, Ho HC. 2013. Live and dead GFP-tagged bacteria showed indistinguishable fluorescence in *Caenorhabditis elegans* gut. J Microbiol 51:367–372. https://doi.org/10.1007/s12275-013-2589-8.
43. Fredlund J, Santos JC, Stévenin V, Weiner A, Latour-Lambert P, Rechav K, Mallet A, Krijnse-Locker J, Elbaum M, Enninga J. 2018. The entry of *Salmonella* in a distinct tight compartment revealed at high temporal and ultrastructural resolution. Cell Microbiol 20:1–13. https://doi.org/10.1111/cmi.12816.
44. Bakkum T, Heemskerk MT, Bos E, Groenewold M, Oikonomeas-Koppasis N, Walburg KV, Van Veen S, Van Der Lienden MJC, Van Leeuwen T, Haks MC, Ottenhoff THM, Koster AJ, Van Kasteren SI. 2020. Bioorthogonal correlative light-electron microscopy of *Mycobacterium tuberculosis* in macrophages reveals the effect of antituberculosis drugs on subcellular bacterial distribution. ACS Cent Sci 6:1997–2007. https://doi.org/10.1021/acscentsci.0c00539.
45. Tam C, LeDue J, Mun JJ, Herzmark P, Robey EA, Evans DJ, Fleiszig SMJ. 2011. 3D quantitative imaging of unprocessed live tissue reveals epithelial defense against bacterial adhesion and subsequent traversal requires MyD88. PLoS One 6:e24008. https://doi.org/10.1371/journal.pone.0024008.
46. Kellermann M, Scharte F, Hensel M. 2021. Manipulation of host cell organelles by intracellular pathogens. Int J Mol Sci 22:6484. https://doi.org/10.3390/ijms22126484.

47. Case EDR, Smith JA, Ficht TA, Samuel JE, De Figueiredo P. 2016. Space: a final frontier for vacuolar pathogens. Traffic 17:461–474. https://doi.org/10.1111/tra.12382.
48. Creasey EA, Isberg RR. 2014. Maintenance of vacuole integrity by bacterial pathogens. Curr Opin Microbiol 17:46–52. https://doi.org/10.1016/j.mib.2013.11.005.
49. Chaudhary A, Miller SI. 2019. Xenophagy: Pathogen-containing vacuoles are hard to digest. Curr Biol 29:R1086–R1088. https://doi.org/10.1016/j.cub.2019.08.069.
50. Rietsch A, Mekalanos JJ. 2006. Metabolic regulation of type III secretion gene expression in *Pseudomonas aeruginosa*. Mol Microbiol 59:807–820. https://doi.org/10.1111/j.1365-2958.2005.04990.x.
51. Meluleni GJ, Grout M, Evans DJ, Pier GB. 1995. Mucoid *Pseudomonas aeruginosa* growing in a biofilm *in vitro* are killed by opsonic antibodies to the mucoid exopolysaccharide capsule but not by antibodies produced during chronic lung infection in cystic fibrosis patients. J Immunol 155:2029–2038.
52. Evans DJ, Allison DG, Brown MRW, Gilbert P. 1991. Susceptibility of *Pseudomonas aeruginosa* and *Escherichia coli* biofilms towards ciprofloxacin: effect of specific growth rate. J Antimicrob Chemother 27:177–184. https://doi.org/10.1093/jac/27.2.177.
53. Nguyen JA, Yates RM. 2021. Better together: current insights into phagosome-lysosome fusion. Front Immunol 12:636078. https://doi.org/10.3389/fimmu.2021.636078.
54. Zolfaghar I, Angus AA, Kang PJ, To A, Evans DJ, Fleiszig SMJ. 2005. Mutation of *retS*, encoding a putative hybrid two-component regulatory protein in *Pseudomonas aeruginosa*, attenuates multiple virulence mechanisms. Microbes Infect 7:1305–1316. https://doi.org/10.1016/j.micinf.2005.04.017.
55. Mikkelsen H, Bond NJ, Skindersoe ME, Givskov M, Lilley KS, Welch M. 2009. Biofilms and type III secretion are not mutually exclusive in *Pseudomonas aeruginosa*. Microbiology (Reading) 155:687–698. https://doi.org/10.1099/mic.0.025551-0.
56. Wu YT, Tam C, Zhu LS, Evans DJ, Fleiszig SMJJ. 2017. Human tear fluid reduces culturability of contact lens-associated *Pseudomonas aeruginosa* biofilms but induces expression of the virulence-associated type III secretion system. Ocul Surf 15:88–96. https://doi.org/10.1016/j.jtos.2016.09.001.
57. Nikaido H. 2009. Multidrug resistance in bacteria. Annu Rev Biochem 78:119–146. https://doi.org/10.1146/annurev.biochem.78.082907.145923.
58. Mah T-F, Pitts B, Pellock B, Walker GC, Stewart PS, O'Toole GA. 2003. A genetic basis for *Pseudomonas aeruginosa* biofilm antibiotic resistance. Nature 426:306–310. https://doi.org/10.1038/nature02122.
59. Masuda N, Ohya S. 1992. Cross-resistance to meropenem, cephems, and quinolones in *Pseudomonas aeruginosa*. Antimicrob Agents Chemother 36:1847–1851. https://doi.org/10.1128/AAC.36.9.1847.
60. Barrett TC, Mok WWK, Murawski AM, Brynildsen MP. 2019. Enhanced antibiotic resistance development from fluoroquinolone persisters after a single exposure to antibiotic. Nat Commun 10:1177. https://doi.org/10.1038/s41467-019-09058-4.
61. Stévenin V, Chang YY, Le Toquin Y, Duchateau M, Gianetto QG, Luk CH, Salles A, Sohst V, Matondo M, Reiling N, Enninga J. 2019. Dynamic growth and shrinkage of the *Salmonella*-containing vacuole determines the intracellular pathogen niche. Cell Rep 29:3958–3973.e7. https://doi.org/10.1016/j.celrep.2019.11.049.
62. Padmanabhan B, Fielden LF, Hachani A, Newton P, Thomas DR, Cho HJ, Ai Khoo C, Stojanovski D, Roy CR, Scott NE, Newton HJ. 2020. Biogenesis of the spacious *Coxiella*-containing vacuole depends on host transcription factors TFEB and TFE3. Infect Immun 88:1–15. https://doi.org/10.1128/IAI.00534-19.
63. Lepanto P, Bryant DM, Rossello J, Datta A, Mostov KE, Kierbel A. 2011. *Pseudomonas aeruginosa* interacts with epithelial cells rapidly forming aggregates that are internalized by a lyn-dependent mechanism. Cell Microbiol 13:1212–1222. https://doi.org/10.1111/j.1462-5822.2011.01611.x.
64. Wang S, Parsek MR, Wozniak DJ, Ma LZ. 2013. A spider web strategy of type IV pili-mediated migration to build a fibre-like Psl polysaccharide matrix in *Pseudomonas aeruginosa* biofilms. Environ Microbiol 15:2238–2253. https://doi.org/10.1111/1462-2920.12095.
65. Williams McMackin EA, Corley JM, Karash S, Marden J, Wolfgang MC, Yahr TL. 2021. Cautionary notes on the use of arabinose- and rhamnose-inducible expression vectors in *Pseudomonas aeruginosa*. J Bacteriol 203:e00224-21. https://doi.org/10.1128/JB.00224-21.
66. Almblad H, Harrison JJ, Rybtke M, Groizeleau J, Givskov M, Parsek MR, Tolker-Nielsen T. 2015. The cyclic AMP-Vfr signaling pathway in *Pseudomonas aeruginosa* is inhibited by cyclic Di-GMP. J Bacteriol 197:2190–2200. https://doi.org/10.1128/JB.00193-15.
67. Robertson DM, Li L, Fisher S, Pearce VP, Shay JW, Wright WE, Cavanagh HD, Jester JV. 2005. Characterization of growth and differentiation in a telomerase-immortalized human corneal epithelial cell line. Invest Ophthalmol Vis Sci 46:470–478. https://doi.org/10.1167/iovs.04-0528.
68. Rybtke MT, Borlee BR, Murakami K, Irie Y, Hentzer M, Nielsen TE, Givskov M, Parsek MR, Tolker-Nielsen T. 2012. Fluorescence-based reporter for gauging cyclic Di-GMP levels in *Pseudomonas aeruginosa*. Appl Environ Microbiol 78:5060–5069. https://doi.org/10.1128/AEM.00414-12.
69. Singer JT, Phennicie RT, Sullivan MJ, Porter LA, Shaffer VJ, Kim CH. 2010. Broad-host-range plasmids for red fluorescent protein labeling of Gram-negative bacteria for use in the zebrafish model system. Appl Environ Microbiol 76:3467–3474. https://doi.org/10.1128/AEM.01679-09.
70. Tam C, Lewis SEE, Li WYY, Lee E, Evans DJJ, Fleiszig S. 2007. Mutation of the phospholipase catalytic domain of the *Pseudomonas aeruginosa* cytotoxin ExoU abolishes colonization promoting activity and reduces corneal disease severity. Exp Eye Res 85:799–805. https://doi.org/10.1016/j.exer.2007.08.015.
71. Lee EJJ, Cowell BAA, Evans DJJ, Fleiszig SMJM. 2003. Contribution of ExsA-regulated factors to corneal infection by cytotoxic and invasive *Pseudomonas aeruginosa* in a murine scarification model. Invest Ophthalmol Vis Sci 44:3892–3898. https://doi.org/10.1167/iovs.02-1302.
72. Jacobs MA, Alwood A, Thaipisuttikul I, Spencer D, Haugen E, Ernst S, Will O, Kaul R, Raymond C, Levy R, Chun-Rong L, Guenthner D, Bovee D, Olson MV, Manoil C. 2003. Comprehensive transposon mutant library of *Pseudomonas aeruginosa*. Proc Natl Acad Sci U S A 100:14339–14344. https://doi.org/10.1073/pnas.2036282100.
73. Urbanowski ML, Brutinel ED, Yahr TL. 2007. Translocation of ExsE into Chinese hamster ovary cells is required for transcriptional induction of the *Pseudomonas aeruginosa* type III secretion system. Infect Immun 75:4432–4439. https://doi.org/10.1128/IAI.00664-07.